IOSUD – ”DUNĂREA DE JOS” UNIVERSITY OF GALATI

Doctoral School of Mechanical and Industrial Engineering

DOCTORAL THESIS

SUMMARY

ANALYSIS OF THE BIOMECHANICAL SYSTEM OF THE DRIVER USING THE KINECT SENSOR

Ph.D. Candidate,

eng. Valentin-Tiberiu AMORȚILĂ

PhD Supervisor,

Prof. dr. eng. Elena MEREUȚĂ

Series I6: Mechanical Engineering No. 52

GALATI

2020

IOSUD - ”DUNĂREA DE JOS” UNIVERSITY OF GALATI

Doctoral School of Mechanical and Industrial Engineering

DOCTORAL THESIS

SUMMARY

ANALYSIS OF THE BIOMECHANICAL SYSTEM OF THE DRIVER USING THE KINECT SENSOR

Ph.D. Candidate

Eng. Valentin-Tiberiu AMORȚILĂ

Chairman of the Scientific Committee,	**Prof. dr. eng. Eugen Victor Cristian RUSU** “Dunarea de Jos” University of Galati
PhD Supervisor,	**Prof. dr. eng. Elena MEREUȚĂ** “Dunarea de Jos” University of Galati
Scientific Committee:	**Prof. dr. eng. Călin Ioan ROŞCA** Transilvania University of Brasov
	Prof. dr. eng. Nicolae BUZBUCHI Maritime University of Constanta
	Assoc. Prof. dr. eng. Doina BOAZU “Dunarea de Jos” University of Galati

Series I6: Mechanical Engineering No. 52
GALAȚI
2020

KEYWORDS: biomechanics, Kinect sensor, driver.

Contents

CHAPTER 1

INTRODUCTION

1.1 MOTIVATION OF CHOOSING THE TOPIC AND THE DOCTORAL THESIS OBJECTIVES

The development of urban areas make the distances that humans are constrained to walk longer and longer. To diminish their movement time and effort, public transport is called for, which, in turn, has a single common element: the human operator. All vehicles entail a human operator who complies to a series of demands during travel. These psychological, physical and intellectual demands generate over time a series of pathological inconveniences and lead to a series of conditions with major consequences to the human body.

The movement of the human body can be quantified on the basis of positional, static, kinetic and dynamic analysis. Thus, optimization technics for locomotion can be proposed, on the principle of strength economy and maximum movement.

The analysis of the driver's movements can lead to the development of novel solutions that have two goals: on the one hand, enhancing the comfort and safeness of the driver and, on the other hand, the optimization of motor vehicles, making them safer, more ergonomical and increasing their performance.

In order to achieve the fundamental objective of this thesis a number of goals were established:

- the analysis of the current status of research involving the usage of specialized systems of video capturing, that allows performing analyses on images;
- the analysis of the geometry of the human movements and of kinetic constraints, identifying kinetic couplers and levers carried out at the level of the skeletal system;
- the implementation of a experimental stand with the aim of reproducing the driver's seat with a view to utilise the Kinect sensor;
- conducting experimental records and specific analyses for kinetic and dynamic analysis of the driver's movements;
- the experimental analysis of positioning the hands on the wheel in order to identify the influence to the reaction time of the driver;
- analysis of the research stage with respect to the field of multibody modeling of the human biomechanical system;
- the identification of mechanical and mathematical models for the sitting posture;
- creation of a mechanical and mathematical model of the driver for the dynamic analysis of the effects of using different devices while driving.

1.4 CURRENT STATE OF RESEARCH CONCERNING THE BIOMECHANICAL SYSTEM OF THE DRIVER

The specialised literature offers recommendations regarding the angles between anatomical elements for the study of the biomechanic of the driver. In the paper: „A literature review on optimum and preferred joint angles in automative sitting posture" [26], the interval ranges of angle variation between the anatomical segments are analysed (figures: 1.19, 1.20, 1.21 and 1.22):

- for ankle joint:

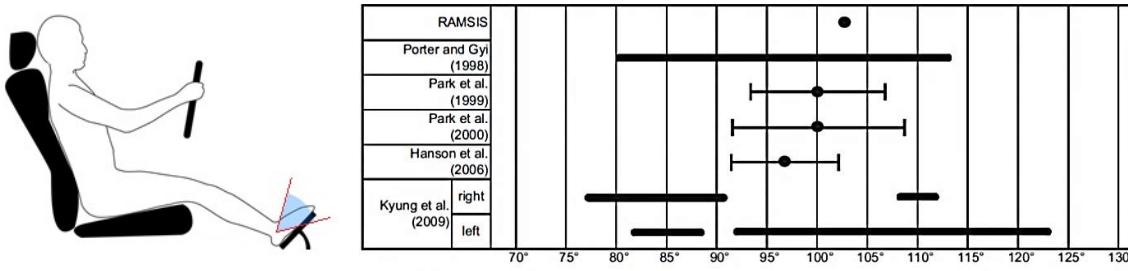

Figure 1. 19. The angles of the ankle joint according to the specialised literature

- for knee joint:

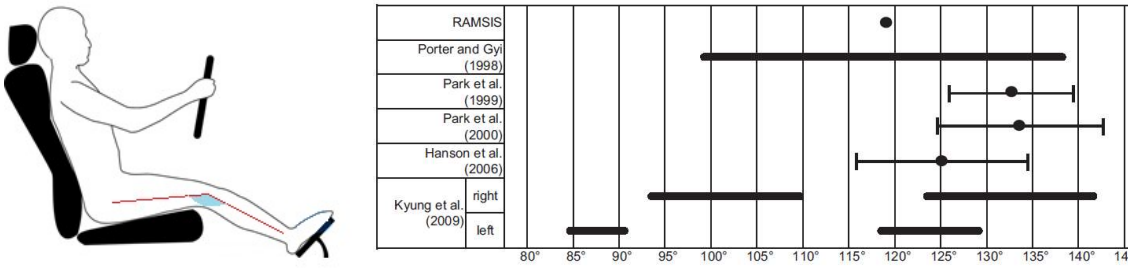

Figure 1. 20. The angles of the ankle joint according to the specialised literature

- for hip joint:

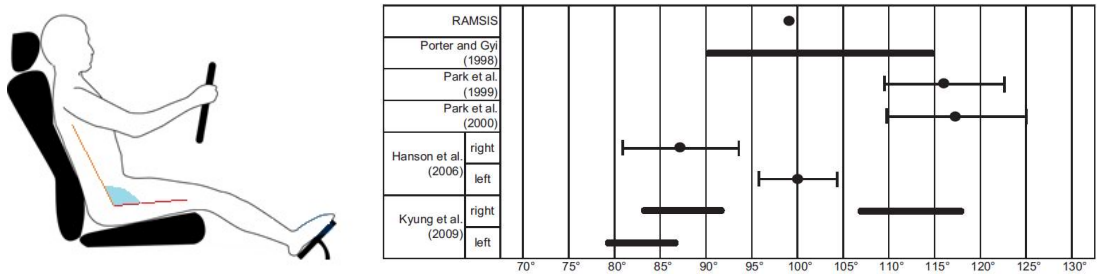

Figure 1. 21. The angles of the hip joint according to the specialised literature

- for shoulder joint:

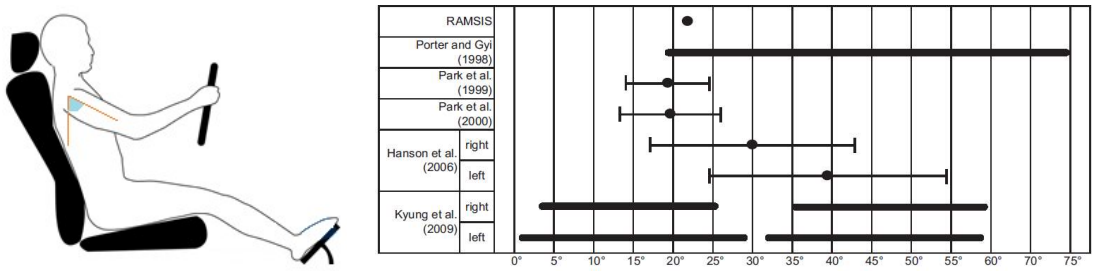

Figure 1. 22. The angles of the shoulder joint according to the specialised literature

1.4.2. BIOMECHANICAL RESEARCHES USING THE KINECT SYSTEM FOR MOTION CAPTURE

A recent study of particular importance in the field of passenger safety who are in road vehicles (figure 1.44) was realised in the year 2017 by Loeb H, Kim J, Arbogast K, Kuo J, Koppel S, Cross S and Charlton J [66]. The study assessed children safety, while road vehicles function using anthropomorphic test devices (ATDs) placed in optimal positions. In this study, the authors examined the feasibility of using the Kinect sensor as well as the analytical algorithms, for recording the positions of children occupying rear seats. The data obtained concludes the fact that, when traveling, passengers who are children are often not in safe positions.

(a) (b) (c)

Figure 1. 44. Automatic recognition of the rear seat occupant's head position using the Kinect depth sensor. (a) The method of implementation of the Kinect sensor (b) The identification of the correct head positions (c) The identification of the incorrect head position [66]

1.5 PARTIAL CONCLUSIONS

In this chapter we have made a general description of the human biomechanical system and an analysis of the current stage of the posture of the human body in order to identify the advantages and limitations of various researches.

Recent studies on the driver's position leading to a series of conclusions:

- kinematic analysis of a single anatomical segment cannot be performed without taking into account the elements that articulate that element and the anatomical kinematic constraints
- it is not possible to speak of a standard position at the wheel, unanimously accepted, because it depends on a number of factors such as, the type of car, the

comfort and design of the seat, the age, the sex of the driver, etc., which directly or indirectly affect the kinematics and / or the dynamics of the driver

- the use of non - invasive methods in biomechanical analysis requires the use of motion capture systems which need to be as accurate as possible and which can provide data sets concerning the acquisition and processing of these methods.

The use of the Kinect motion capture system finds its applicability during the biomechanical analysis, through a correct identification of different anatomical features and joints for the analysis of the spatial - temporal motion parameters. Through the option of creating a virtual mechanical skeleton of the subject under analysis, the Kinect sensor offers the possibility of a kinetic and dynamic analysis without using optic markers.

CHAPTER 2

METHODS AND INSTRUMENTS FOR BIOMECHANICAL ANALYSIS OF THE DRIVER

The precise analysis of positional parameters of the human body is of paramount importance in the research of various domains and in their transposition in the virtual reality. The need for motion capture has made it necessary to develop technologies that can capture the position and play it back using the computer [82]. The accuracy of the experimental measurements has increased along with the development of the technique and the adoption of modern means of investigation in the movement analysis.

2.2 OPTICAL EQUIPMENT FOR MOTION CAPTURE USED IN THE DOCTORAL THESIS – THE KINECT SENSOR

In order to capture the human movement without attaching markers, sensors or other devices to the human body, hardware systems have been developed that can detect, track and display the elements of the human anatomical system [85].

The Kinect device tracks the movements and gestures of the subjects and provides data on the position of the joints of the human kinetic chains in the 3D coordinate system.

2.2.1 KINECT SENSOR - HARDWARE COMPONENTS

The Kinect sensor was launched with the aim of capturing movement for the Xbox video console, but has found its use in other areas due to the its ease of interacting with the subject.

Figure 2. 3. The image capture cameras of the Kinect sensor [86]

Capturing depth data is done through a PrimeSense microchip that transmits a signal to the infrared transmitter to generate infrared light (1) and another signal to the IR depth sensor to initiate the capture of depth data from the sensor capture area (2). At the same time,

the IR transmitter emits another ray in the infrared spectrum, invisible (3), towards the capture area found in front of the device. The IR depth sensor initiates the reading of the reflected points in the object (4) and sends them to the PrimeSense microchip (5) which in turns analyses them and generates a depth image on the frame (6). The operating scheme is shown in Figure 2.7.

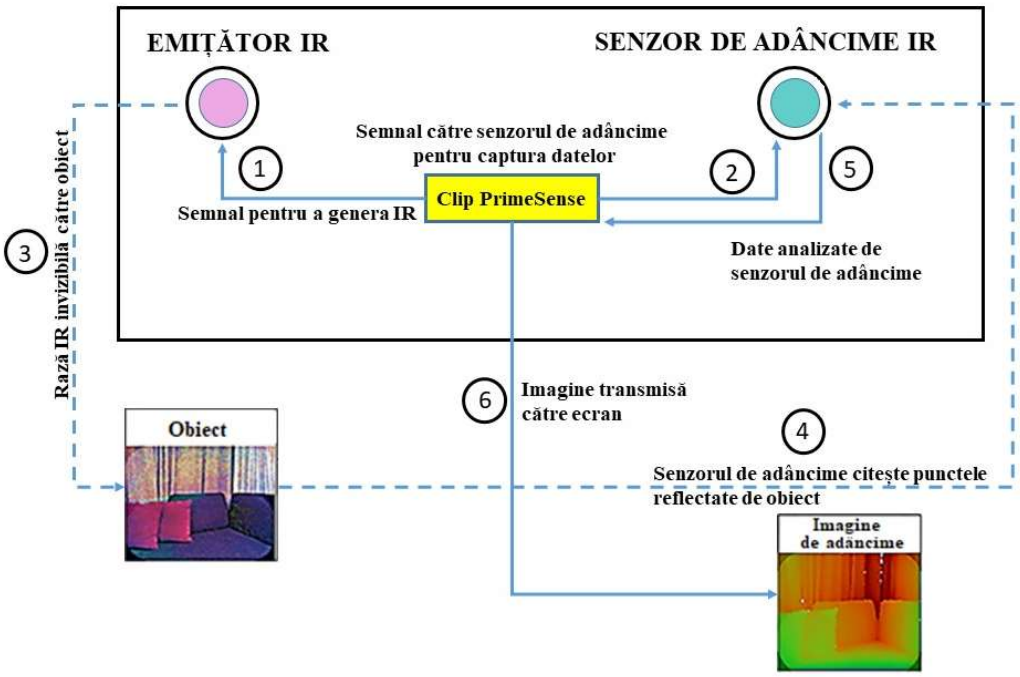

Figure 2. 7. The operating scheme of the PrimeSense technology [87]

2.3 PROFESSIONAL SOFTWARES FOR MOVEMENT ANALYSIS

2.3.1 KINOVEA – SOFTWARE FOR BIOMECHANICAL ANALYSIS OF THE INDEPENDENT MOVEMENTS

Most frequently used software applications for the analysis of human movements are the applications that offer the advantage of further processing of the video signal obtained from the various professional image capture systems. Such a software application is Kinovea which allows a two - dimensional analysis of a video recording regardless of the capture system utilised.

Kinovea is a video analysing software that allows the capture and playback, at different speeds, of a video recording, with the possibility to analyse a series of kinematic parameters. Kinovea was created especially for the analysis of various movements in different sports, in order to improve sports performance, but also for postural rehabilitation or correction [94], [95].

2.3.2 USING THE iPi SOFT - APPLICATION IN THE BIOMECHANICAL ANALYSIS

iPi Motion Capture was developed as a tool for tracking and recording 3D movements of the human body, for the purpose of 3D animation (figure 2.13). This software allows the connection (with the purpose of recording and processing) of video cameras equipped with depth sensors or motion controllers, offering the possibility of transferring data in several common formats. iPi Motion Capture offers a package of modules needed for recording and processing data:

- iPi Recorder 4.0 software (30-day free software offered by iPi Soft) provides real-time tracking allowing to capture and play back recordings.
- To process the video scenes through which movement is transferred into 3D characters, the iPi Mocap Studio software is used.This software (free 30-day software offered by iPi Soft) uses an integrated technology that allows the automatic transfer of movement to a custom platform, identifying the bones and joints of the human body, translating them into kinematic elements and couplings [97].

2.3.3 DESIGN OF AN EXPERIMENTAL STAND SIMILAR TO THE DRIVING PLACE

The experimental stand created reproduces the driving position of an Opel vehicle and was realized within the Engineering Faculty of the "Dunărea de Jos", University in Galați. The dimensions of the driver's seat were measured and reproduced exactly, and for the driver's seat a real seat of a similar car was used.

Figure 2. 23. Designed car stand - made

2.4 PARTIAL CONCLUSIONS

Optical recording systems have an important contribution to the motion capture and analysis. For this reason, it is intended that in the analysis of a biomechanical system, a device with a simple interface will be used, indicating the movements and allowing the comparison with an existing model in a data library for its correction or optimization.

The Kinect sensor has the disadvantage of a low resolution when the video capture is made three-dimensional. The small number of points for which triangulation is obtained leads to some less precise approximations. Also, the impossibility of tracking the subject when an object interposes between it and the sensor or when the pursuit of the subject is obstructed by another anatomical element.

The advantages offered by video capture systems for biomechanical analysis involve adapting them according to the purpose pursued. Thus, for the biomechanical analysis of the driver with the help of the Kinect sensor, it was necessary to create a car stand that reproduces the driving position and which offers the optimum conditions for registration. In this chapter we presented the design and construction of this stand.

CHAPTER 3

STRUCTURAL IDENTIFICATION OF THE BIOMECHANICAL SYSTEM OF THE DRIVER

The driver's position represents a limited work position where the driver must interact and operate with the vehicle controls to interact and operate with the vehicle controls. The limiting constraints are the result of the space occupied by the driver and by the placement of various devices that must be acted upon. The driver's anthropometric and biomechanical characteristics influence the kinematic chains in which the anatomical elements are constituted for a certain one motion.

3.1 DRIVER'S ANATOMICAL LEVERS

I reduced the spine and the other anatomical elements to a system of rigid articulated bars to identify all the levers of the biomechanical system of the driver (figure. 3.2).

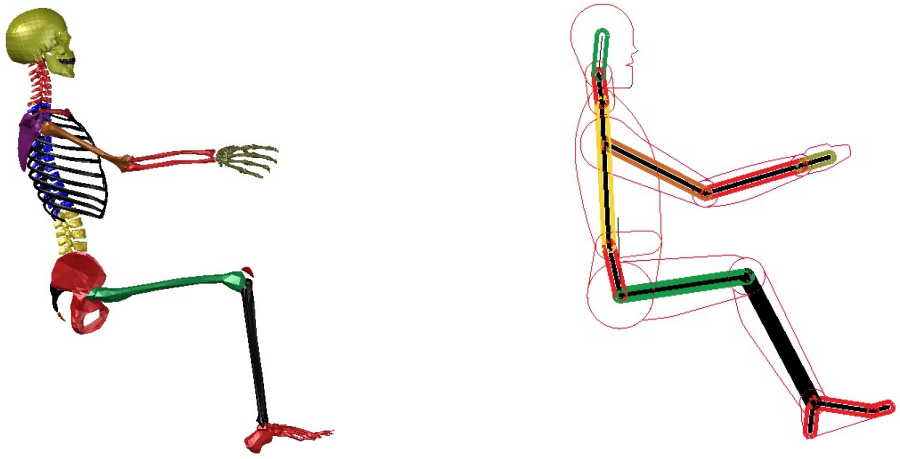

Figure 3. 2. The transformation of the bone system into a system of rigid articulated bars

3.2 DRIVER'S ANATOMICAL JOINTS

3.2.9. METATARSOPHALANGEAL JOINTS OF THE LEG

The arrangement of the bone segments and the joints at the level of the foot respects the hand's structure, except that the haloes do not have the same mobility and cannot execute the movement of opposition. The metatarsal - phalangeal joint behaves like a fifth - class kinematic couple, allowing a single rotational movement (figure 3.21).

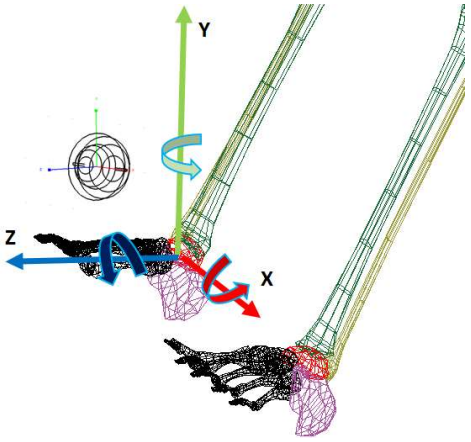

Figure 3. 20. The ankle joint – third-class kinematic coupling

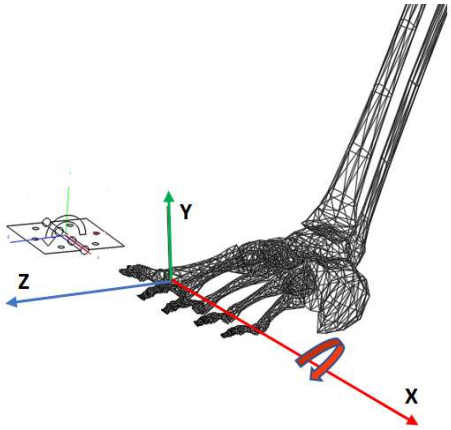

Figure 3. 21. The metatarsal - phalangeal joint - fifth-class kinematic coupling

3.4 THE PARAMETRIC EQUATIONS OF THE CONFIGURATION AND KINEMATICS OF JOINTS ON THE PEDAL ACTION

The analysis of the kinematic chain of the driver can be approached by inverse kinematics (the position of the effector element is known, more precisely the position of the phalangeal joint with the metatarsals) or by direct kinematics (the coordinates of the other joints are known and the position of the drive segment is determined) (figure 3.26).

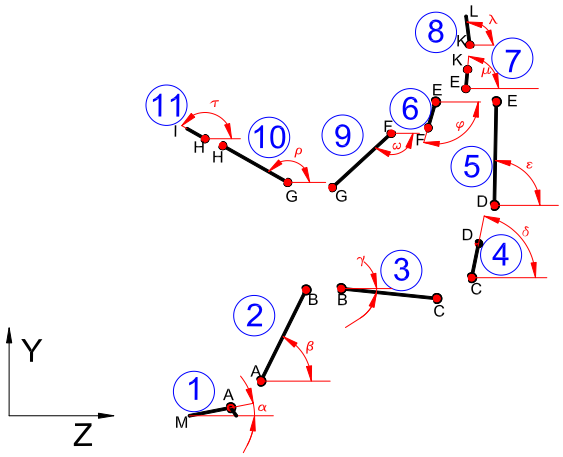

Figure 3. 26. The kinematic model in the sagittal plane of the driver

Based on the anthropometric data of the driver (by inverse kinematics) the coordinates of the ankle, knee, hip, spine, shoulder, elbow, hand, neck and head can be determined. If we consider the lengths of the anatomical elements and their absolute angles as in figure 3.26 based on the inverse kinematics, we obtain the following parametric equations:

$$z_A = z_M + l_1 \cos\alpha \tag{3.3}$$
$$y_A = y_M + l_1 \sin\alpha \tag{3.4}$$
$$z_B = z_A + l_2 \cos\beta = z_M + l_1 \cos\alpha + l_2 \cos\beta \tag{3.5}$$
$$y_B = y_A + l_2 \sin\beta = y_M + l_1 \sin\alpha + l_2 \sin\beta \tag{3.6}$$
$$z_C = z_B + l_3 \cos\gamma = z_M + l_1 \cos\alpha + l_2 \cos\beta + l_3 \cos\gamma \tag{3.7}$$
$$y_C = y_B + l_3 \sin\gamma = y_M + l_1 \sin\alpha + l_2 \sin\beta + l_3 \sin\gamma \tag{3.8}$$
$$\ldots\ldots\ldots\ldots\ldots\ldots\ldots\ldots\ldots\ldots\ldots\ldots\ldots\ldots\ldots\ldots\ldots\ldots\ldots\ldots\ldots\ldots\ldots\ldots$$
$$z_I = z_H + l_{11}\cos\tau = z_M + l_1\cos\alpha + l_2\cos\beta + l_3\cos\gamma + l_4\cos\delta + l_5\cos\varepsilon + l_6\cos\varphi + l_7\cos\mu + l_8\cos\lambda + l_9\cos\omega + l_{10}\cos\rho + l_{11}\cos\tau \tag{3.9}$$
$$y_I = y_H + l_{11}\sin\tau = y_M + l_1\sin\alpha + l_2\sin\beta + l_3\sin\gamma + l_4\sin\delta + l_5\sin\varepsilon + l_6\cos\varphi + l_7\sin\mu + l_8\sin\lambda + l_9\sin\omega + l_{10}\sin\rho + l_{11}\sin\tau \tag{3.10}$$

If we generalize the equations 3.3 - 3.10, we obtain the following parametric equations of the joints:

$$z_k = z_M + \sum_{k=1}^{11} l_k \cos\theta \tag{3.11}$$
$$y_k = y_M + \sum_{k=1}^{11} l_k \sin\theta \tag{3.12}$$

The movement speeds of the joints on the Oz and Oy axes can be determined as it follows:

$$\dot{z}_A = \dot{z}_M - l_1\omega_1 \sin\alpha \tag{3.13}$$
$$\dot{y}_A = \dot{y}_M + l_1\omega_1 \cos\alpha \tag{3.14}$$
$$\dot{z}_B = \dot{z}_A - l_2\omega_2 \sin\beta = \dot{z}_M - l_1\omega_1 \sin\alpha - l_2\omega_2 \sin\beta \tag{3.15}$$
$$\dot{y}_B = \dot{y}_A + l_2\omega_2 \cos\beta = \dot{y}_M + l_1\omega_1 \cos\alpha + l_2\omega_2 \cos\beta \tag{3.16}$$
$$\dot{z}_C = \dot{z}_B - l_3\omega_3 \sin\gamma = \dot{z}_M - l_1\omega_1 \sin\alpha - l_2\omega_2 \sin\beta - l_3\omega_3 \sin\gamma \tag{3.17}$$
$$\dot{y}_C = \dot{y}_B + l_3\omega_3 \cos\gamma = \dot{y}_M + l_1\omega_1 \cos\alpha + l_2\omega_2 \cos\beta + l_3\omega_3 \cos\gamma \tag{3.18}$$

……

Thus, the general equation of the linear speed of movement of the joint will be:

$$\dot{z}_k = \dot{z}_M - \sum_{k=1}^{11} l_k \omega_k \sin\theta \tag{3.19}$$

$$\dot{y}_k = \dot{y}_M + \sum_{k=1}^{11} l_k \omega_k \cos\theta \tag{3.20}$$

Analog, for accelerations we obtain:

$$\ddot{z}_k = \ddot{z}_M - \sum_{k=1}^{11} l_k \varepsilon_k \sin\theta - \sum_{k=1}^{11} l_k \omega_k^2 \cos\theta \tag{3.21}$$

$$\ddot{y}_k = \ddot{y}_M + \sum_{k=1}^{11} l_k \varepsilon_k \cos\theta - \sum_{k=1}^{11} l_k \omega_k^2 \sin\theta \tag{3.22}$$

3.5 KINEMATIC ANALYSIS OF THE LOWER LIMB BIOMECHANIC CHAIN WHEN THE CLUTCH PEDAL IS PRESSED, USING THE KINOVEA SOFTWARE

Used as a motion analysis software for performance athletes, Kinovea offers the possibility to capture data for cinematic analysis.

3.5.1 VIDEO RECORDING FOR KINEMATIC ANALYSIS

The video recording was realized with a 1920 x 1080 pixel resolution camera. The pilot mark was set at 100 mm and was mounted on the side of the seat backrest, and the marked joints, with a 10 x 10 mm marker are: the ankle joint, the knee joint and the hip joint (figure 3.27). Also, the pelvis and metatarsals were marked. The dimensions of the elements in the two positions were calculated automatically by the application. Figure 3.27 shows a variation of the length of the elements due to the elasticity of the article of clothing (max. 310 μm).

Figure 3. 27. Calibration and dimensioning of the elements

From the large number of video recordings, two consecutive actuations of the clutch pedal were selected, after the subject had settled with the pedal.

3.5.3 THE ANALYSIS OF THE KINEMATIC PARAMETERS OF THE DRIVER

The car manufacturers intend to provide sufficient space for the movement of the anatomical elements during the maneuvers, without limiting the movement.

The horizontal and vertical movement of the biomechanical system of the lower limb analyzed is given by the positions that the joints occupy at a certain moment (figure 3.33a and figure 3.33b). It can be noticed that in the case of ”no heel" the horizontal displacement of the joints is divided almost equally between flexion and extension. In the case of ”heel", flexion 1 takes 0.630 seconds, and the ankle joint begins to move in front of the other joints. The distance realized by the ankle joint in the ”heel” case is about 30 mm longer than the ”no heel” ankle, due to the initial position of the lower limb. The movements in the case of „heel" are shaken, there is no horizontal movement synchronized between the three joints [100].

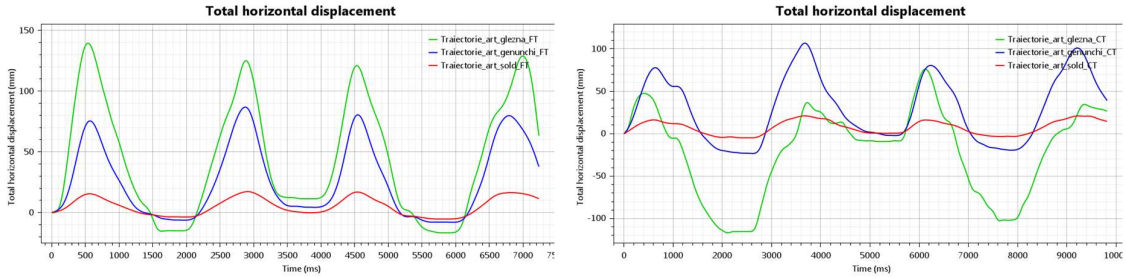

(a) (b)

Figure 3. 33. Horizontally moving joints (a) without heel (b) with heel

The linear speed in the ”no heel” case, when the lower limb is free (flexion 1 and extension 2) exceeds 0,5 m / s, while in the other case this speed does not exceed 0,4 m / s (figure 3.35a and 3.35b). The maximum speed during operation (extension 1 and flexion 2) is approximately equal in both cases.

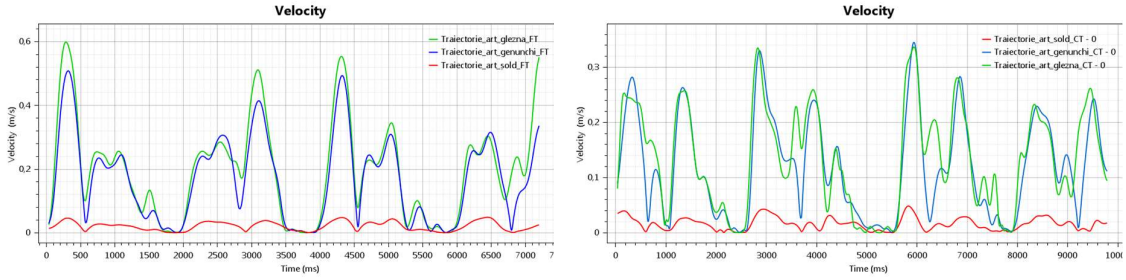

(a) (b)

Figure 3. 35. Linear speed of joints (a) without heel (b) with heel

As a result of the analysis, it is found that between the angles of the ”no heel” joints is a better correlation than in the other case studied (figure 3.40). The greatest correlation is found between the angles of the driver's hip and knee. In both cases, this correlation indicates that the flexions and extensions of the driver's knee are in close connection.

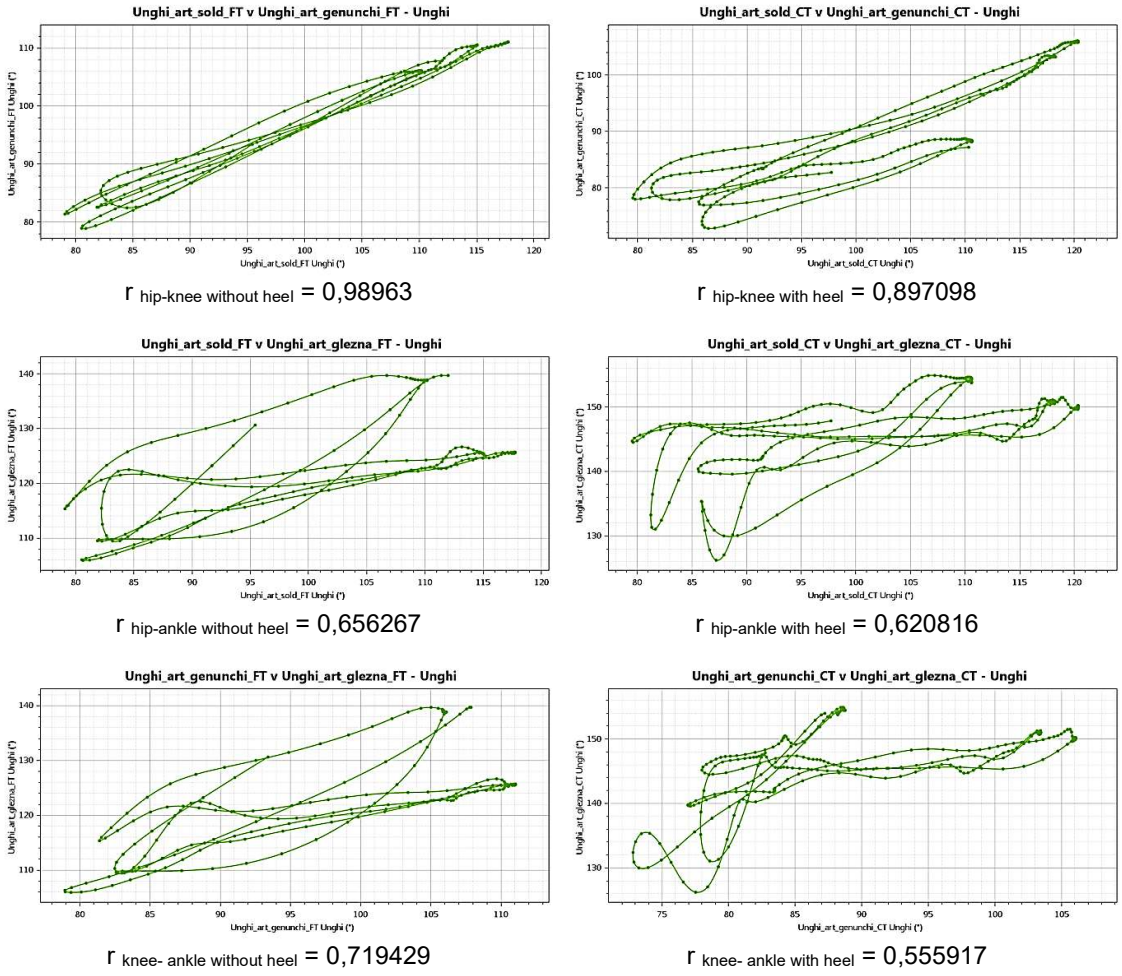

Figure 3. 40. The correlation between the angles of the joints of the lower limb

A high plantar pressure in the heel and metatarsal head areas can lead to postural abnormalities. Analyzing the pressure and the plantar surfaces, it was concluded that the high plantar arch and the hyperextension of the toes lead to a high pressure associated with a decrease of the plantar support area, thus with postural instability [101].

3.6 EXPERIMENTAL STUDY ON THE INFLUENCE OF HAND POSITIONING (ON THE STEERING WHEEL) ON THE TEMPERATURE

3.6.1 ANALYSIS OF THE HAND POSITIONING ON THE STEERING WHEEL

The experiment consisted of measuring the temperature of the hands on the steering wheel in 3 different positions (zones ”10 – 2”, ”9 – 3” and ”7 - 5") of the time dial.

The measurement time was 300 s, during which the subjects kept both hands on the steering wheel in each of the”10 – 2”, ”9 – 3” and ”7 – 5” zones. Between the measurements of each position, breaks of at least 5 minutes were made for thermoregulation of the hands’ temperature. The temperature data of both hands were collected in all areas subject to analysis

at 10 s intervals. Statistical data analysis was performed using a spreadsheet program (Office - Excel).

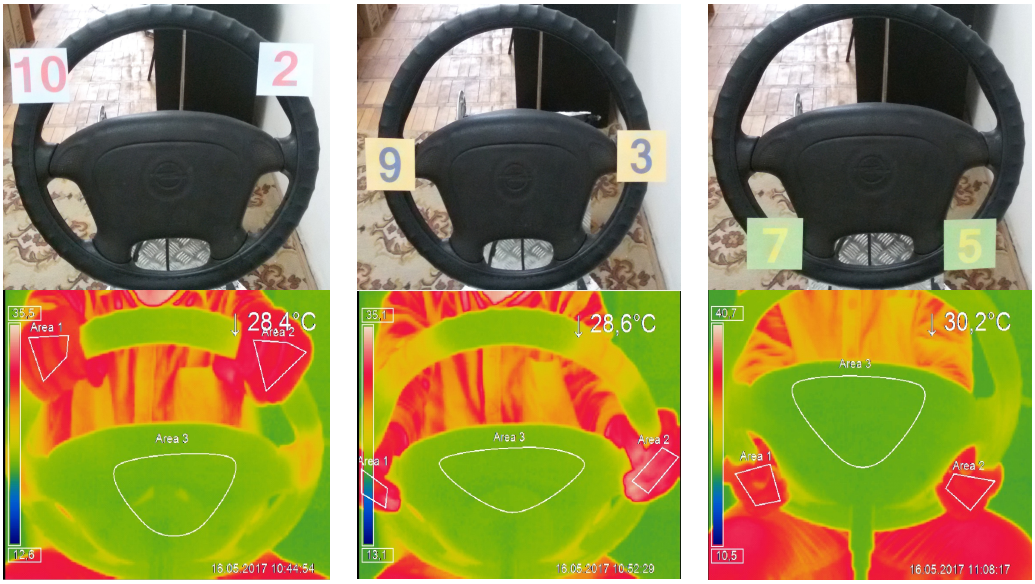

Figure 3. 44. The positions of the hands in the thermally measured areas

Thus, in the position ”10 – 2”, a decrease in the temperature of the hands with values between 0.8 ° C and 2.3 ° C is observed in all subjects (figure 3.45).

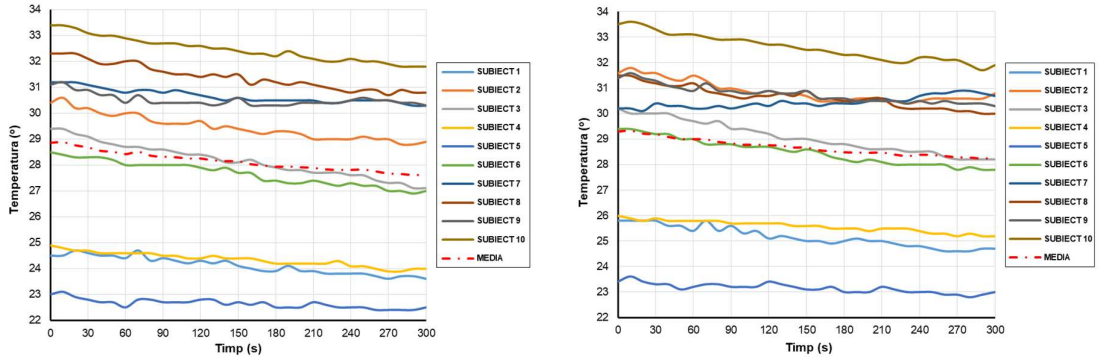

(a) (b)

Figure 3. 45. Variation of the temperature of the hands and the average of the temperatures in the area ”10 – 2” (a) the right hand (b) the left hand

For the position of the hands in the area ”9 – 3”, it is found that the temperatures of the hands do not register the same values in all subjects. For most cases, the temperature is kept around the initial temperature (figure 3.46). Significant variation is recorded in subjects 5 and 8, with an increase in the temperature of the right hand of 3.9 ° C and, respectively, 5 ° C. It is observed that for 60% of the subjects, the temperature of the dorsal surface of the left hand decreases with values between 0,3 ° C and 0,9 ° C, and for 40% of the subjects, the temperature increases with values between 0,2 ° C and 4.1 ° C. Also, the average temperature of all subjects recorded an increase of about 0.51 ° C in the right hand and about 0.26 ° C in the left hand.

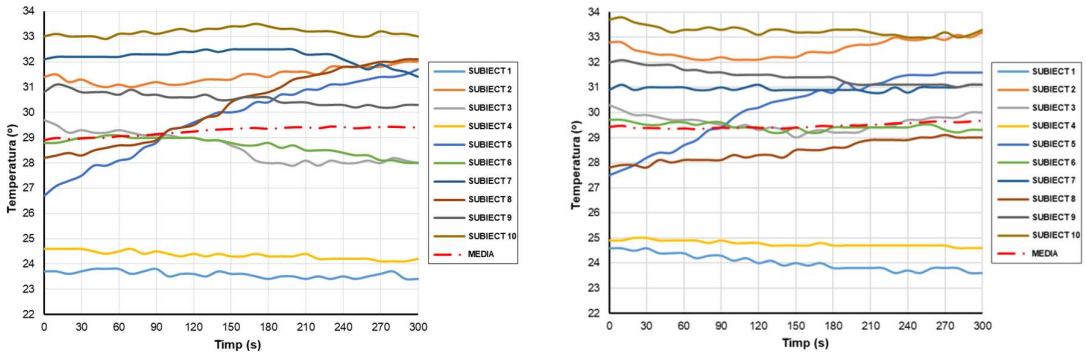

(a) (b)

Figure 3. 46. Variation of the temperature of the hands and the average temperature in the area ”9 – 3” (a) the right hand (b) the left hand

3.8 PARTIAL CONCLUSIONS

A motion capture system was used to capture the real-time position of key points of the driver's body during a specified action.

Following the thermal analysis of the temperature of the hands in different positions on the steering wheel in static mode, the following conclusions can be drawn:

- positioning the hands in the area "10 - 2" is the most unfavorable point; from the point of view of blood circulation, which is why, in all subjects, the temperature decreases, with a linear tendency, having a strong correlation with the average;
- placing the hands in position "7 - 5" proves to be more favorable, from a thermal point of view, compared to the positioning in the area "10 - 2", the slope of the regression equations being smaller, but it represents an uncomfortable position from the point of view of the comfort and kinematics of the hands;
- the thermal analysis of the hands in the position "9 - 3" proved to be the best, the temperature variations being insignificant for 5 minutes, considering that these variations are due to the heat exchange with the outside and the thermoregulation at the finger level.

The tendency of drivers to position their hands in the "10 - 2" area and the exposure to problems of coordination or the syndrome of white fingers (Raynaud) can be solved by adopting by the car manufacturers the models of steering wheel used in Formula 1, or the existing steering wheel with heating system.

CHAPTER 4

STRESS ANALYSIS OF THE DRIVER BIOMECHANICAL SYSTEM

4 .1 SKELETIC MUSCLES ROLE

The active part of the locomotor system is the muscles that have the role of generating forces acting on the skeleton. Myology is the science that deals with the study of muscles and their attachments, that is, the muscular system. Muscles are differentiated organs, contractile and elastic that, following an excitation, contract, producing a mechanical work:

- if the request is static (holding a post) the muscle performs a static mechanical work;
- at a dynamic request (when the movement occurs) the muscle responds with a dynamic mechanical work.

4.2.1 MUSCULAR FORCE

The muscular force, generated by the muscular contractions, depends on two variables, the length and the tension of the muscle:

- when the muscle contraction is isometric, the variation of the muscle tension does not change the length of the muscle;
- an isotonic contraction of the muscles does not change the muscle tension throughout the contraction;
- if the length of the muscle is shortened, the contraction is concentric;
- if the length of the muscle increases, the contraction is eccentric.

The mode of production of the net force that shortens the length of the muscle fiber is realized through complex anatomical processes, but, from the mechanical point of view, the generation of this force is the result of the difference between the active and the resistive force [122]. If this difference has a positive value, the movement occurs (figure 4.4).

Figure 4. 4. The scheme of the production of the motion that is generated by the muscles

4.3 EXPERIMENT CONCERNING BIOMECHANICAL ANALYSIS OF THE DRIVER USING THE KINECT SENSOR AND THE iPi SOFT APPLICATION

The experiment consisted of recording the movements of the driver and processing the video recordings in order to determine the trajectories, speeds and accelerations of the mass centers of 11 anatomical elements from the sagittal plane (foot, leg, thigh, hip, lumbar area, scapular area, neck, head, arm, forearm and hand). These anatomical elements are the most significant for the biomechanical analysis of the driver.

For the position of the driver, a car stand that reproduces the driver's driving position (presented in chapter 2) was used. The recording was done with the help of 2 Kinect sensors that were disposed at 120 ° to the capture area and at a height of 1.5 m above the ground. The two Kinect sensors were connected on the same interface.

4.3.1 EXPERIMENTAL RESULTS OF THE FLEXION AND EXTENSION OF THE LEFT FOOT ON THE CLUTCH PEDAL OPERATION

Following the trajectories of the 11 elements subjected to the analysis for actuating the clutch pedal, we find that:

- their displacement on the Ox (transverse axis of the seat) has small values, about 8 mm, insensible; the highest values are recorded at the level of the left foot, 114 mm, due to the fact that it generates the movement;
- the movement on the Oy axis (the axis on the height) of the elements is conditioned by the height of the pedal, which is why the maximum value of the movement is registered at the foot level of 110 mm;
- depth movement, following the Oz axis (longitudinal axis of the car), has observable values at all levels, the minimum value is recorded by hand, about 10 mm, and the maximum value at the left foot of 132 mm.

The recorded values of the speed of movement of the 11 studied elements (figure 4.11) lead to the conclusion that the anatomical effector elements, the foot and the leg, have the highest speeds.

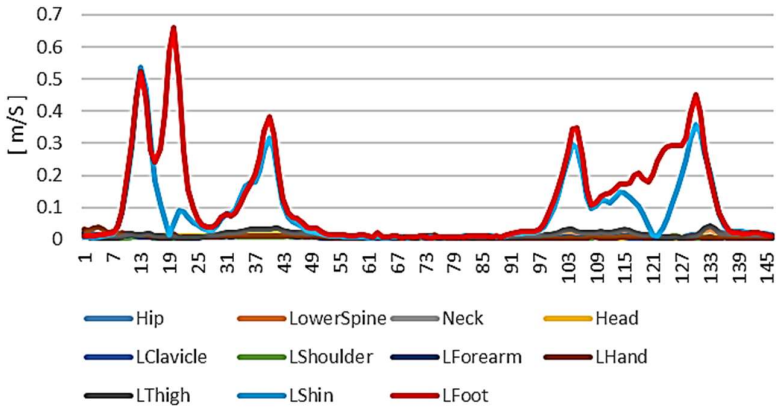

Figure 4. 11. The speed of movement of the elements when actuating the clutch pedal

The accelerations of the elements record maximum values at the level of the foot and leg. The four compound movements for which the left foot acceleration reaches the maximum

value of 6.73 m / s2 at frame 21 during flexion 1 are observed on the acceleration graph (figure 4.13).

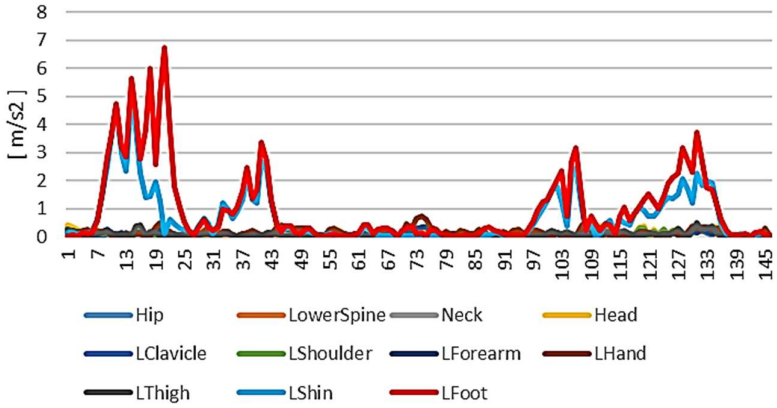

Figure 4. 13. The acceleration of the elements when operating the clutch pedal

Analyzing the net forces developed at the level of the anatomical elements during the operation of the clutch with the left foot (Fig. 4.15), it is observed that high values are obtained at the level of the lower limb, at the leg about 21.84 N and at the foot approximately 9.28 N, but also in the lower area of the lumbar spine, about 10.95 N.

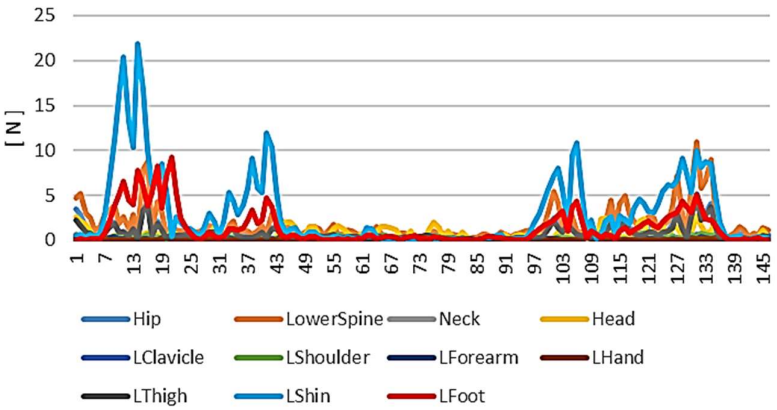

Figure 4. 15. The net forces developed by the anatomical elements of the driver when driving the clutch pedal

At the lumbar area there is a high value of the net force, due to the fact that the muscle groups in this area develop a resting force, necessary to maintain the upper body posture [125]. The highest values of the net force variation are obtained at the level of the leg muscle group, as a generator element of movement and at the lower level of the spine.

Following the analysis of the forces at the level of the 11 anatomical elements, it was observed that in the sacral-lumbar area (lower spine) large forces of the muscle groups in this area develop as a result of maintaining the body in the sitting position. To see if there is a connection between the action of the muscle groups responsible for the flexion - extension movement of the lower left limb when applying the clutch pedal and the muscles of the lumbar area, we statistically analyzed the correlation between the forces of the 11 elements using the Pearson coefficient.

Thus, it is observed in figure 4.17 that there is a strong correlation between the forces developed in the lumbar area and the forces in the hip, thigh area, and with the forces of the leg muscle group a moderate correlation. It can be said that the forces developed by the lower left limb when operating the clutch pedal influence the lumbar area.

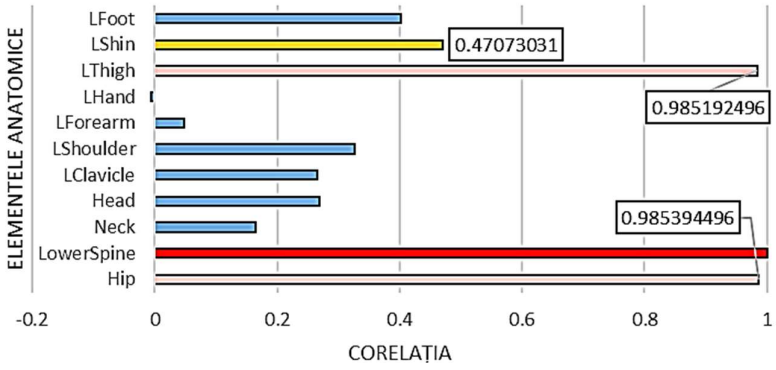

Figure 4. 17. Pearson correlation between the forces developed in the lumbar area and the forces developed in the other anatomical elements

4.4 PARTIAL CONCLUSIONS

In order to determine if during the four movements by the driver there is a connection between the action of the muscle groups in the lumbar - sacral area and the forces developed at the level of the other 10 anatomical elements, using the Pearson coefficient we statistically analyzed the correlation between these and it can be concluded that:

- • the forces developed by the lower left limb when actuating the clutch pedal influence the lumbar area;
- • when operating the brake pedal, the forces developed by the muscle groups at the level of the hip and thigh have a strong correlation with the forces in the lumbar area;
- • in the case of turning the steering wheel to the left with 90 ° the correlation between the force at the lumbar level and the forces responsible for the movement of the head and neck is a moderate correlation; the correlation between the force generated by the muscle group responsible for the movement of the hand and the force in the lumbar area is weak - moderate;
- • the correlation between the forces in the lumbar spine area and the forces developed by the right arm when rotating the steering wheel to the right is small to moderate; a moderate influence is registered with the muscular forces at the level of the right clavicle and of the hip area.

CHAPTER 5

DRIVER'S DYNAMICS

5.4 PROPOSED DYNAMIC MODEL OF THE DRIVER

The proposed model is composed of 11 elements connected with elastic and dissipative systems connected in parallel (Voight model) that reproduce the important muscle groups responsible for the main movements of the driver (flexion - extension of the lower limbs, internal and external rotation of the upper limbs)(figure 5.8). The 11 anatomical elements, modeled as a mass - spring – damping (MSD), represent the most significant parts of the human body that participate and influence its movement in the driving position of a car [129], [130], [131].

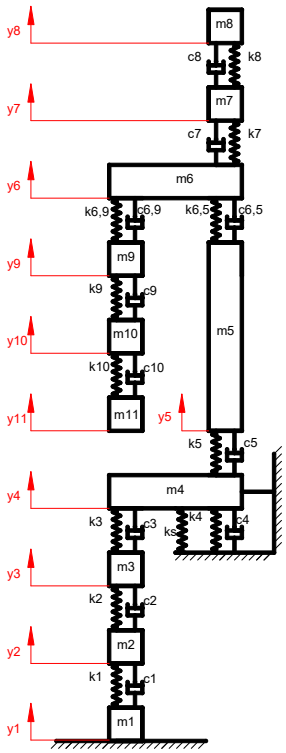

Figure 5. 8. The model of the driver for analyzing the behavior of the muscle groups when operating the pedals and the steering wheel

5.5 ESTABLISHING THE MOVEMENT EQUATIONS OF THE ELEMENTS MASS – SPRING - DAMPER

The equation that models the dynamic behavior of the system is [26]:

$$[M]\{\ddot{Y}\}+[C]\{\dot{Y}\}+[K]\{Y\}=\{F\} \tag{5.11}$$

where:

- [M] – represents the matrix of inertia (of the masses),
- [C] - represents the matrix of the depreciation coefficients,
- [K] - represents the matrix of the stiffness coefficients,
- $\{\ddot{Y}\}$ – the vector of accelerations,
- $\{\dot{Y}\}$ – velocity vector,
- $\{Y\}$ – the displacement vector.

The proposed mathematical model falls into the category of multivariable mechanical systems whose equations can be written as follows:

$$\begin{cases} m_1\cdot\ddot{y}_1+c_1\cdot\dot{y}_1+k_1\cdot y_1=m_1\cdot g \\ m_2\cdot\ddot{y}_2+c_2\cdot(\dot{y}_2-\dot{y}_1)+k_2\cdot(y_2-y_1)-c_1\cdot\dot{y}_1-k_1\cdot y_1=m_2\cdot g \\ m_3\cdot\ddot{y}_3+c_3\cdot(\dot{y}_3-\dot{y}_2)+k_3\cdot(y_3-y_2)-c_2\cdot(\dot{y}_2-\dot{y}_1)-k_2\cdot(y_2-y_1)=m_3\cdot g \\ m_4\cdot\ddot{y}_4+c_5\cdot(\dot{y}_5-\dot{y}_4)+k_5\cdot(y_5-y_4)-k_3\cdot(y_3-y_2)-c_3\cdot(\dot{y}_3-\dot{y}_2)-k_s\cdot y_4-k_4\cdot(y_4-y_3)-c_4\cdot(\dot{y}_4-\dot{y}_3)=m_4\cdot g \\ m_5\cdot\ddot{y}_5+c_{65}\cdot(\dot{y}_6-\dot{y}_5)+k_{65}\cdot(y_6-y_5)-c_5\cdot(\dot{y}_5-\dot{y}_4)-k_5\cdot(y_5-y_4)=m_5\cdot g \\ m_6\cdot\ddot{y}_6+c_7\cdot(\dot{y}_7-\dot{y}_6)+k_7\cdot(y_7-y_6)-c_{65}\cdot(\dot{y}_6-\dot{y}_5)-k_{65}\cdot(y_6-y_5)-k_{69}\cdot(y_6-y_9)-c_{69}\cdot(\dot{y}_6-\dot{y}_9)=m_6\cdot g \\ m_7\cdot\ddot{y}_7+c_8\cdot(\dot{y}_8-\dot{y}_7)+k_8\cdot(y_8-y_7)-c_7\cdot(\dot{y}_7-\dot{y}_6)-k_7\cdot(y_7-y_6)=m_7\cdot g \\ m_8\cdot\ddot{y}_8-c_8\cdot(\dot{y}_8-\dot{y}_7)-k_8\cdot(y_8-y_7)=m_8\cdot g \\ m_9\cdot\ddot{y}_9+c_{69}\cdot(\dot{y}_6-\dot{y}_9)+k_{69}\cdot(y_6-y_9)-c_9\cdot(\dot{y}_9-\dot{y}_{10})-k_9\cdot(y_9-y_{10})=m_9\cdot g \\ m_{10}\cdot\ddot{y}_{10}+c_9\cdot(\dot{y}_9-\dot{y}_{10})+k_9\cdot(y_9-y_{10})-c_{10}\cdot(\dot{y}_{10}-\dot{y}_{11})-k_{10}\cdot(y_{10}-y_{11})=m_{10}\cdot g \\ m_{11}\cdot\ddot{y}_{11}+c_{10}\cdot(\dot{y}_{10}-\dot{y}_{11})+k_{10}\cdot(y_{10}-y_{11})=m_{11}\cdot g \end{cases} \tag{5.12}$$

in which:

- m_i – the masses of the elements;
- c_i – damping coefficients (dissipative);
- k_i – stiffness coefficients.

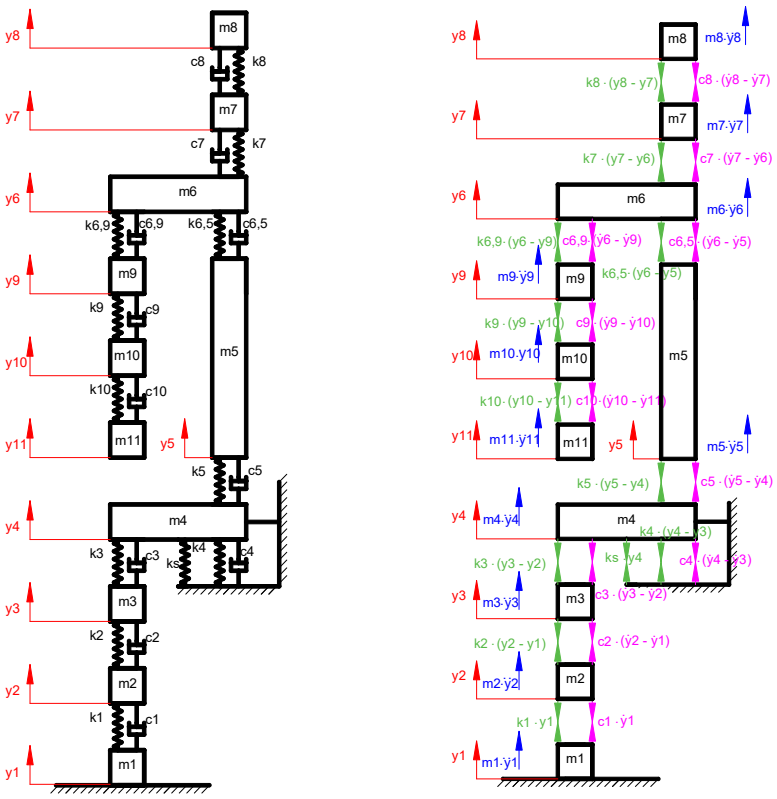

Figura 5. 9. The forces acting on the biomechanical system along the Oy axis

The matrix form of the system (5.12) is:

$$\begin{bmatrix} m_1 & 0 & 0 & 0 & 0 & 0 & 0 & 0 & 0 & 0 & 0 \\ 0 & m_2 & 0 & 0 & 0 & 0 & 0 & 0 & 0 & 0 & 0 \\ 0 & 0 & m_3 & 0 & 0 & 0 & 0 & 0 & 0 & 0 & 0 \\ 0 & 0 & 0 & m_4 & 0 & 0 & 0 & 0 & 0 & 0 & 0 \\ 0 & 0 & 0 & 0 & m_5 & 0 & 0 & 0 & 0 & 0 & 0 \\ 0 & 0 & 0 & 0 & 0 & m_6 & 0 & 0 & 0 & 0 & 0 \\ 0 & 0 & 0 & 0 & 0 & 0 & m_7 & 0 & 0 & 0 & 0 \\ 0 & 0 & 0 & 0 & 0 & 0 & 0 & m_8 & 0 & 0 & 0 \\ 0 & 0 & 0 & 0 & 0 & 0 & 0 & 0 & m_9 & 0 & 0 \\ 0 & 0 & 0 & 0 & 0 & 0 & 0 & 0 & 0 & m_{10} & 0 \\ 0 & 0 & 0 & 0 & 0 & 0 & 0 & 0 & 0 & 0 & m_{11} \end{bmatrix} \cdot \begin{Bmatrix} \ddot{y}_1 \\ \ddot{y}_2 \\ \ddot{y}_3 \\ \ddot{y}_4 \\ \ddot{y}_5 \\ \ddot{y}_6 \\ \ddot{y}_7 \\ \ddot{y}_8 \\ \ddot{y}_9 \\ \ddot{y}_{10} \\ \ddot{y}_{11} \end{Bmatrix}$$

$$+$$

$$\begin{bmatrix} c_1 & 0 & 0 & 0 & 0 & 0 & 0 & 0 & 0 & 0 & 0 \\ -(c_1+c_2) & c_2 & 0 & 0 & 0 & 0 & 0 & 0 & 0 & 0 & 0 \\ c_2 & -(c_2+c_3) & c_3 & 0 & 0 & 0 & 0 & 0 & 0 & 0 & 0 \\ 0 & c_3 & (c_4-c_3) & -c_5 & c_5 & 0 & 0 & 0 & 0 & 0 & 0 \\ 0 & 0 & 0 & c_5 & -(c_{65}+c_5) & c_{65} & 0 & 0 & 0 & 0 & 0 \\ 0 & 0 & 0 & 0 & c_{65} & -(c_{65}+c_{69}+c_7) & c_7 & 0 & c_{69} & 0 & 0 \\ 0 & 0 & 0 & 0 & 0 & c_7 & -(c_7+c_8) & c_8 & 0 & 0 & 0 \\ 0 & 0 & 0 & 0 & 0 & 0 & c_8 & -c_8 & 0 & 0 & 0 \\ 0 & 0 & 0 & 0 & 0 & c_{69} & 0 & 0 & -(c_{69}+c_9) & c_9 & 0 \\ 0 & 0 & 0 & 0 & 0 & 0 & 0 & 0 & c_9 & -(c_9+c_{10}) & c_{10} \\ 0 & 0 & 0 & 0 & 0 & 0 & 0 & 0 & 0 & c_{10} & -c_{10} \end{bmatrix} \cdot$$

$$\begin{Bmatrix} \dot{y}_1 \\ \dot{y}_2 \\ \dot{y}_3 \\ \dot{y}_4 \\ \dot{y}_5 \\ \dot{y}_6 \\ \dot{y}_7 \\ \dot{y}_8 \\ \dot{y}_9 \\ \dot{y}_{10} \\ \dot{y}_{11} \end{Bmatrix}$$

+

$$\begin{bmatrix} k_1 & 0 & 0 & 0 & 0 & 0 & 0 & 0 & 0 & 0 & 0 \\ -(k_1+k_2) & k_2 & 0 & 0 & 0 & 0 & 0 & 0 & 0 & 0 & 0 \\ k_2 & -(k_2+k_3) & k_3 & 0 & 0 & 0 & 0 & 0 & 0 & 0 & 0 \\ 0 & k_3 & k_4-k_3 & -(k_5+k_s) & k_5 & 0 & 0 & 0 & 0 & 0 & 0 \\ 0 & 0 & 0 & k_5 & -(k_5+k_{65}) & k_{65} & 0 & 0 & 0 & 0 & 0 \\ 0 & 0 & 0 & 0 & k_{65} & -(k_{65}+k_{69}+k_7) & k_7 & 0 & k_{69} & 0 & 0 \\ 0 & 0 & 0 & 0 & 0 & k_7 & -(k_7+k_8) & k_8 & 0 & 0 & 0 \\ 0 & 0 & 0 & 0 & 0 & 0 & k_8 & -k_8 & 0 & 0 & 0 \\ 0 & 0 & 0 & 0 & 0 & k_{69} & 0 & 0 & -(k_9+k_{69}) & k_9 & 0 \\ 0 & 0 & 0 & 0 & 0 & 0 & 0 & 0 & k_9 & -(k_9+k_{10}) & k_{10} \\ 0 & 0 & 0 & 0 & 0 & 0 & 0 & 0 & 0 & k_{10} & -k_{10} \end{bmatrix} \cdot$$

$$\begin{Bmatrix} y_1 \\ y_2 \\ y_3 \\ y_4 \\ y_5 \\ y_6 \\ y_7 \\ y_8 \\ y_9 \\ y_{10} \\ y_{11} \end{Bmatrix} = \begin{Bmatrix} m_1 \\ m_2 \\ m_3 \\ m_4 \\ m_5 \\ m_6 \\ m_7 \\ m_8 \\ m_9 \\ m_{10} \\ m_{11} \end{Bmatrix} \cdot (g)$$

If we take into account that the two movements, on Oy and Oz, are realized at the same time then the system of equations becomes:

$$\begin{cases} \sum F_y = 0 \\ \sum F_z = 0 \end{cases} \tag{5.14}$$

Under these conditions the two systems of equations (5.12) and (5.13) are transformed into a single system of 22 equations whose unknowns are the coefficients of rigidity and the coefficients of damping. The rest of the variables are known, being generated by biomechanical analysis using the "iPi soft" software through the "iPi Biomech" module, namely: acceleration, speed, displacement.

To solve the displacement system with 22 equations and 22 unknowns, we developed 3 applications in the Matlab programming language. The first application (Annex 2) aims to read data from iPi Soft in * .xls format. We have created * .mat databases for each of the 10 subjects and for each movement. The parameters contained in the databases belonging to each anatomical element are displacement, speed, acceleration and mass. The second script (Annex 3) aims to solve the system and create a matrix containing the results for the stiffness and damping (dissipative) coefficients of the muscles for different values of the coefficient k_s. The third script (Annex 4) aims to verify the resulting data.

5.6 RESULTS OF MODELING THE DRIVER BIOMECHANICAL SYSTEM

The proposed mathematical model aimed to determine the coefficients of elasticity and damping of the muscle groups of the 11 essential anatomical elements that participate in the operation of the different devices while driving the vehicle. These coefficients were determined for the clutch pedal actuation movement. The mathematical processing for the dynamic identification was done based on the data provided by the tracking of the elements without markers.

Thus, for k_s 2000 N / m it is found that at the level of the sacral-lumbar area the elastic coefficients, k_4, have the highest value causing a high elastic force (figure 5.11). Large values were also determined at the thigh level, k_3, justified by the muscle group responsible for the movement of the lower limb when pedaling. These muscles are the largest of the human body, and the origin and / or insertion are in the pelvic area.

(a)

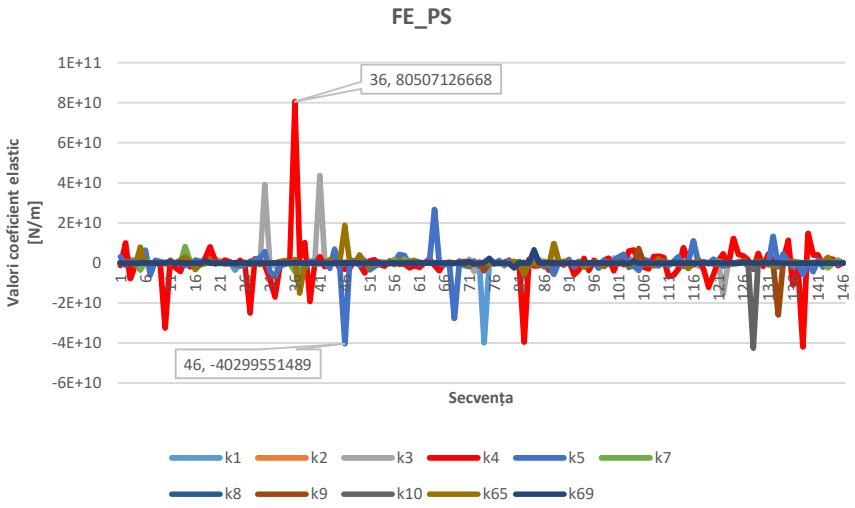

(b)

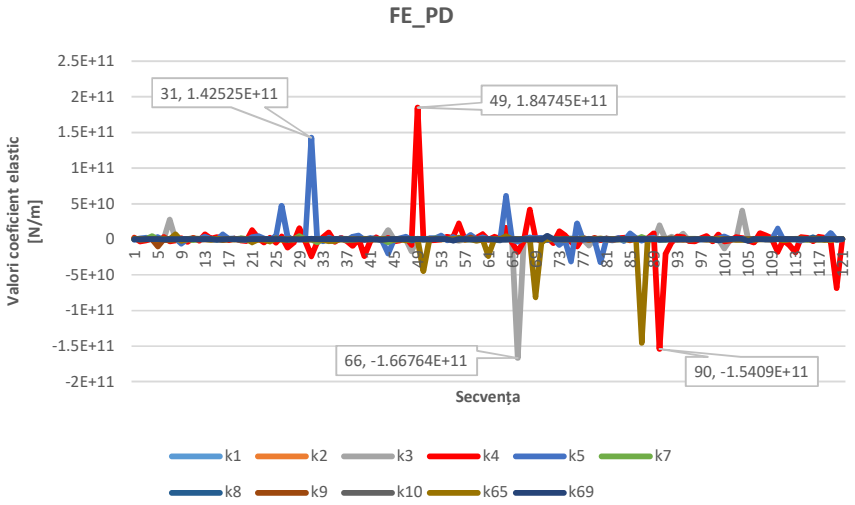

(c)

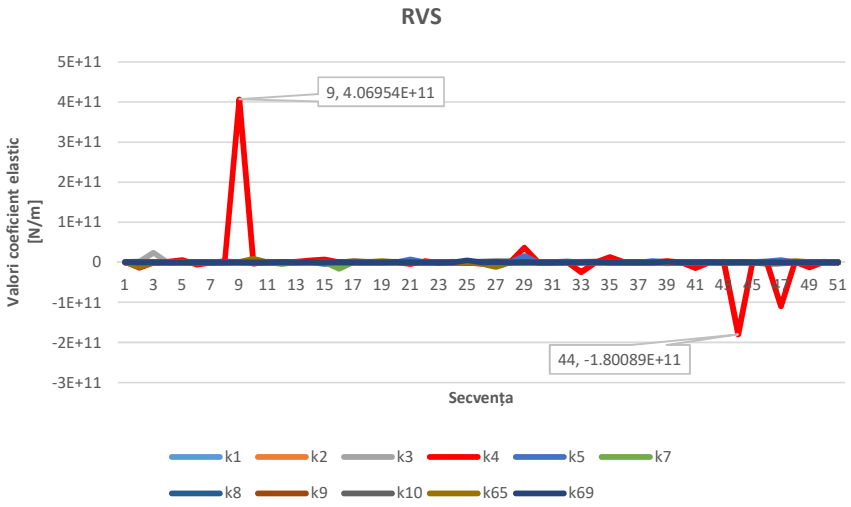

(d)

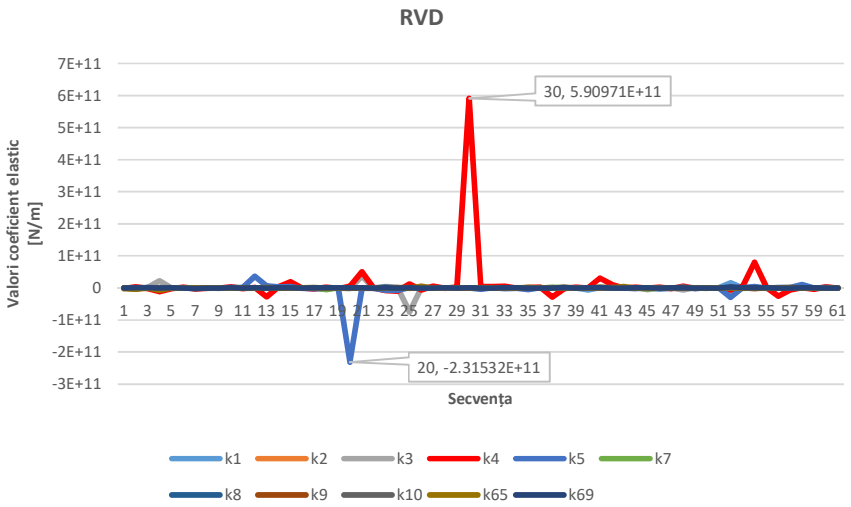

Figure 5. 11. The coefficients of elasticity determined on the mathematical model for ks = 2000 N / m (a) during flexion - extension of the left foot (b) during flexion - extension of the right leg (c) during rotation of the steering wheel to the left (d) during turning the steering wheel to the right

At the dissipative level, the muscle groups dampen in proportion to the elastic forces. High values of the dissipative coefficients were determined in the area of the pelvic girdle in response to the large elastic forces. It is found that in order to achieve the net force, the active force is moderated by the action of the antagonistic muscle group as well as by the viscous rubbing at the muscular level. The high values of the damping and elasticity coefficients are justified by small displacements of the elements in a short time (approximately 33 ms).

All the determined values of the elasticity and damping coefficients for k_s = 2000 N / m are presented as algebraic solutions of solving the system of equations. In reality, these coefficients cannot have negative values, the sign being given by the direction and the sense of the force developed at the muscular level. Annex 5 presents the values of the elasticity and damping coefficients of the muscle groups of the 11 anatomical elements analyzed in absolute value for values of the damping coefficient of the seat, k_s, 250 N / m, 500 N / m and 1000 N / m. It is found that for these values the elasticity and damping coefficients change only at the

lumbar area, the other coefficients of the muscle groups remaining unchanged. It is also found that the highest values of these coefficients are also recorded at the lumbar level.

5.7 REDEFINDING THE DRIVER POSITION

The results obtained based on the model proposed in subchapter 5.6, but also the complexity of the muscular system in the pelvic - sacral and lumbar area, caused me to develop a new model of the dynamic system of the driver. It is observed in figure 5.13 that in the pelvic area the muscles have a triangular connection (psoas between the spine and the femur, the lumbar square between the column and the pelvis, and the iliac muscle between the pelvis and the femur).

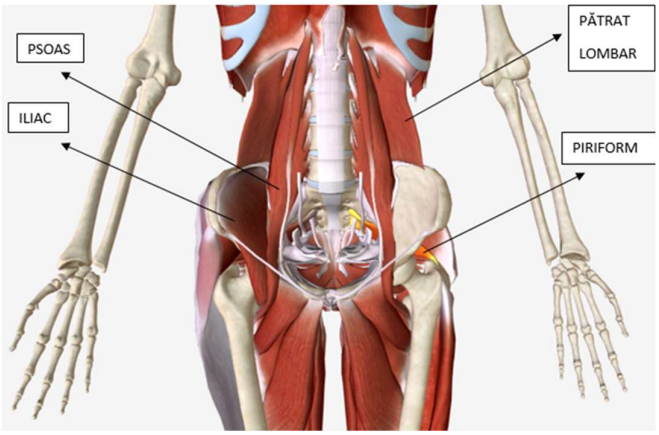

Figure 5. 13. Muscles in the pelvic area with origins and insertions arranged in a triangle

The new model proposed is also composed of 11 rigid elements, but more accurately reproduces the mass - spring - damping system in the pelvis area. At the same time, we also modified the elasticity coefficient of the seat, k_s, considering a rigid seat with elasticity coefficients close to the rubber (10^6 N/m and 10^7 N/m). The new model has the particularity that the rigid element m_3 (thigh) is connected by the element m_5 (spine - sacrum) and m_4 (pelvis). Also, the element m4 (pelvis) is connected with the element m_5 (sacred) (figure 5.14).

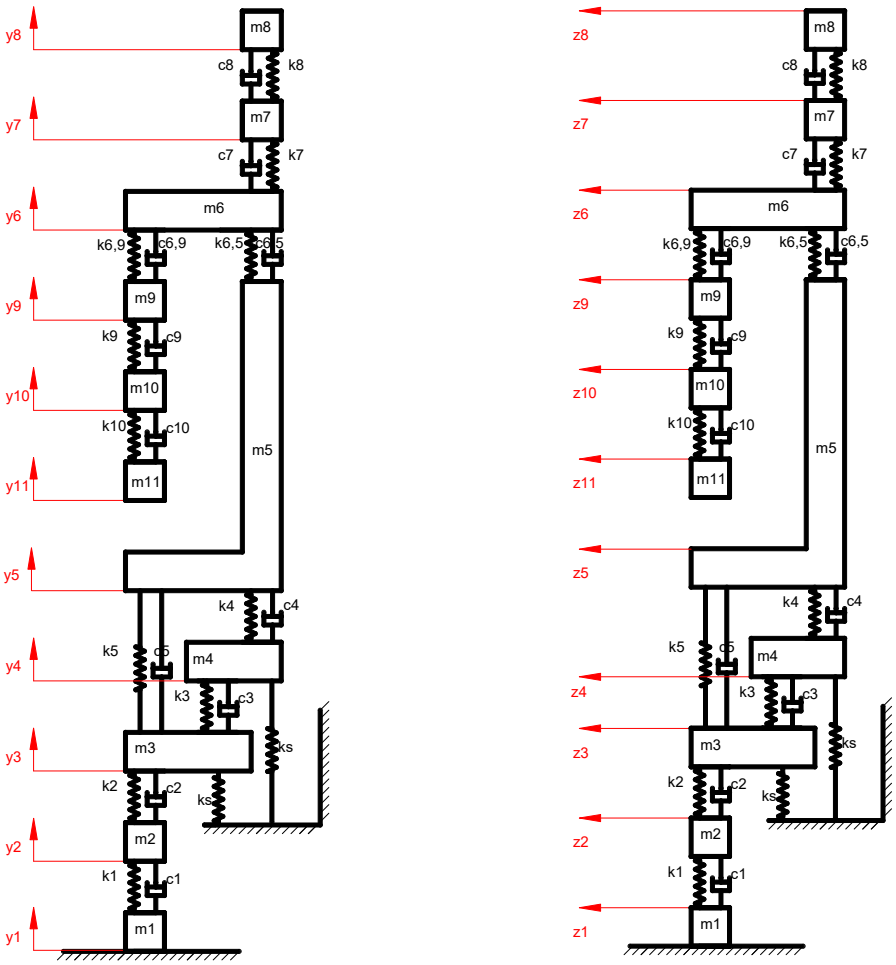

Figure 5. 14. Driver's new mass – spring - damping model

I restarted the experiment on the biomechanical analysis of the driver using the Kinect sensor and the application "iPi- Soft" on 10 clinically healthy subjects without motor deficiencies, between the ages of 20 and 48, holders of driving licenses. The experiment was not invasive and was conducted with the written consent of the subjects to be able to disseminate the results obtained for scientific purposes. Subjects were asked to position themselves on the car stand and perform the same four movements (clutch pedal drive, brake pedal drive, 90° steering wheel to the left and right. The experiment was conducted at an average ambient temperature of 19°C - 22°C without other atmospheric factors intervening. After processing, we obtained the data obtained for the proposed new mathematical model.

The mathematical model of the new configuration fits into multivariable mechanical systems, and the system of equations associated with this model is:

$$\begin{cases} m_1 \cdot \ddot{y}_1 + c_1 \cdot \dot{y}_1 + k_1 \cdot y_1 = m_1 \cdot g \\ m_2 \cdot \ddot{y}_2 - (c_1 + c_2) \cdot \dot{y}_1 + c_2 \cdot \dot{y}_2 - (k_1 + k_2) \cdot y_1 + k_2 \cdot y_2 = m_2 \cdot g \\ m_3 \cdot \ddot{y}_3 + c_2 \cdot \dot{y}_1 - c_2 \cdot \dot{y}_2 - (c_{34} + c_{35}) \cdot \dot{y}_3 + c_{34} \cdot \dot{y}_4 + c_{35} \cdot \dot{y}_5 + k_2 \cdot y_1 - k_2 \cdot y_2 - (k_{34} + k_{35} + k_s) \cdot y_3 + k_{34} \cdot y_4 + k_{35} \cdot y_5 = m_3 \cdot g \\ m_4 \cdot \ddot{y}_4 + c_{34} \cdot \dot{y}_3 - (c_{34} + c_4) \cdot \dot{y}_4 + c_4 \cdot \dot{y}_5 + k_{34} \cdot y_3 - (k_{34} + k_4 + k_s) \cdot y_4 + k_4 \cdot y_5 = m_4 \cdot g \\ m_5 \cdot \ddot{y}_5 + c_{35} \cdot \dot{y}_3 + c_4 \cdot \dot{y}_4 - (c_{65} + c_{35} + c_4) \cdot \dot{y}_5 + c_{65} \cdot \dot{y}_6 + k_{35} \cdot y_3 + k_4 \cdot y_4 - (k_{65} + k_{35} + k_4) \cdot y_5 + k_{65} \cdot y_6 = m_5 \cdot g \\ m_6 \cdot \ddot{y}_6 + c_{65} \cdot \dot{y}_5 - (c_{69} + c_{65} + c_7) \cdot \dot{y}_6 + c_7 \cdot \dot{y}_7 + c_{69} \cdot \dot{y}_9 + k_{65} \cdot y_5 - (k_{69} + k_{65} + k_7) \cdot y_6 + k_7 \cdot y_7 + k_{69} \cdot y_9 = m_6 \cdot g \\ m_7 \cdot \ddot{y}_7 + c_7 \cdot \dot{y}_6 - (c_8 + c_7) \cdot \dot{y}_7 + c_8 \cdot \dot{y}_8 + k_7 \cdot y_6 - (k_7 + k_8) \cdot y_7 + k_8 \cdot y_8 = m_7 \cdot g \\ m_8 \cdot \ddot{y}_8 + c_8 \cdot \dot{y}_7 - c_8 \cdot \dot{y}_8 + k_8 \cdot y_7 - k_8 \cdot y_8 = m_8 \cdot g \\ m_9 \cdot \ddot{y}_9 + c_{69} \cdot \dot{y}_6 - (c_{69} + c_9) \cdot \dot{y}_9 + c_9 \cdot \dot{y}_{10} + k_{69} \cdot y_6 - (k_{69} + k_9) \cdot y_9 + k_9 \cdot y_{10} = m_9 \cdot g \\ m_{10} \cdot \ddot{y}_{10} + c_9 \cdot \dot{y}_9 - (c_9 + c_{10}) \cdot \dot{y}_{10} + c_{10} \cdot \dot{y}_{11} + k_9 \cdot y_9 - (k_9 + k_{10}) \cdot y_{10} + k_{10} \cdot y_{11} = m_{10} \cdot g \\ m_{11} \cdot \ddot{y}_{11} + c_{10} \cdot \dot{y}_{10} - c_{10} \cdot \dot{y}_{11} + k_{10} \cdot y_{10} - k_{10} \cdot y_{11} = m_{11} \cdot g \\ m_1 \cdot \ddot{z}_1 + c_1 \cdot \dot{z}_1 + k_1 \cdot z_1 = 0 \\ m_2 \cdot \ddot{z}_2 - (c_1 + c_2) \cdot \dot{z}_1 + c_2 \cdot \dot{z}_2 - (k_1 + k_2) \cdot z_1 + k_2 \cdot z_2 = 0 \\ m_3 \cdot \ddot{z}_3 + c_2 \cdot \dot{z}_1 - c_2 \cdot \dot{z}_2 - (c_{34} + c_{35}) \cdot \dot{z}_3 + c_{34} \cdot \dot{z}_4 + c_{35} \cdot \dot{z}_5 + k_2 \cdot z_1 - k_2 \cdot z_2 - (k_{34} + k_{35}) \cdot z_3 + k_{34} \cdot z_4 + k_{35} \cdot z_5 = 0 \\ m_4 \cdot \ddot{z}_4 + c_{34} \cdot \dot{z}_3 - (c_{34} + c_4) \cdot \dot{z}_4 + c_4 \cdot \dot{z}_5 + k_{34} \cdot y_3 - (k_{34} + k_4) \cdot z_4 + k_4 \cdot z_5 = 0 \\ m_5 \cdot \ddot{z}_5 + c_{35} \cdot \dot{z}_3 + c_4 \cdot \dot{z}_4 - (c_{65} + c_{35} + c_4) \cdot \dot{z}_5 + c_{65} \cdot \dot{z}_6 + k_{35} \cdot z_3 + k_4 \cdot z_4 - (k_{65} + k_{35} + k_4) \cdot z_5 + k_{65} \cdot z_6 = 0 \\ m_6 \cdot \ddot{z}_6 + c_{65} \cdot \dot{z}_5 - (c_{69} + c_{65} + c_7) \cdot \dot{z}_6 + c_7 \cdot \dot{z}_7 + c_{69} \cdot \dot{z}_9 + k_{65} \cdot z_5 - (k_{69} + k_{65} + k_7) \cdot z_6 + k_7 \cdot z_7 + k_{69} \cdot z_9 = 0 \\ m_7 \cdot \ddot{z}_7 + c_7 \cdot \dot{z}_6 - (c_8 + c_7) \cdot \dot{z}_7 + c_8 \cdot \dot{z}_8 + k_7 \cdot z_6 - (k_7 + k_8) \cdot z_7 + k_8 \cdot z_8 = 0 \\ m_8 \cdot \ddot{z}_8 + c_8 \cdot \dot{z}_7 - c_8 \cdot \dot{z}_8 + k_8 \cdot z_7 - k_8 \cdot z_8 = 0 \\ m_9 \cdot \ddot{z}_9 + c_{69} \cdot \dot{z}_6 - (c_{69} + c_9) \cdot \dot{z}_9 + c_9 \cdot \dot{z}_{10} + k_{69} \cdot z_6 - (k_{69} + k_9) \cdot z_9 + k_9 \cdot z_{10} = 0 \\ m_{10} \cdot \ddot{z}_{10} + c_9 \cdot \dot{z}_9 - (c_9 + c_{10}) \cdot \dot{z}_{10} + c_{10} \cdot \dot{z}_{11} + k_9 \cdot z_9 - (k_9 + k_{10}) \cdot z_{10} + k_{10} \cdot z_{11} = 0 \\ m_{11} \cdot \ddot{z}_{11} + c_{10} \cdot \dot{z}_{10} - c_{10} \cdot \dot{z}_{11} + k_{10} \cdot z_{10} - k_{10} \cdot z_{11} = 0 \end{cases} \quad (5.17)$$

The system was solved using the parameters ($\ddot{y}_i, \dot{y}_i, y_i, \ddot{z}_i, \dot{z}_i, z_i,$) provided by the "iPi - Soft" application and the anthropometric data for the recalculation of the stiffness coefficients (k_i) and the damping coefficients (c_i). To solve the system, we used the MatLab calculation software and a series of applications we developed presented in annexes 2, 3 and 4 of this thesis. The data thus obtained (stiffness coefficients and damping coefficients) were used in a neural network in order to optimize the input values so as to obtain minimum values for the elasticity coefficient of the pelvic area muscle group (k_4).

5.7.1 ARTIFICIAL NEURONAL NETWORK GENERAL CARACTERISTICS

The biological neuron (figure 5.15a) represents a cell specialized in the reception and transmission of information. Through the connections that biological neurons make between them, complex structures such as the human brain are created. By mathematical abstraction of the biological neuron a model was obtained - the perceptron (figure 5.15b).

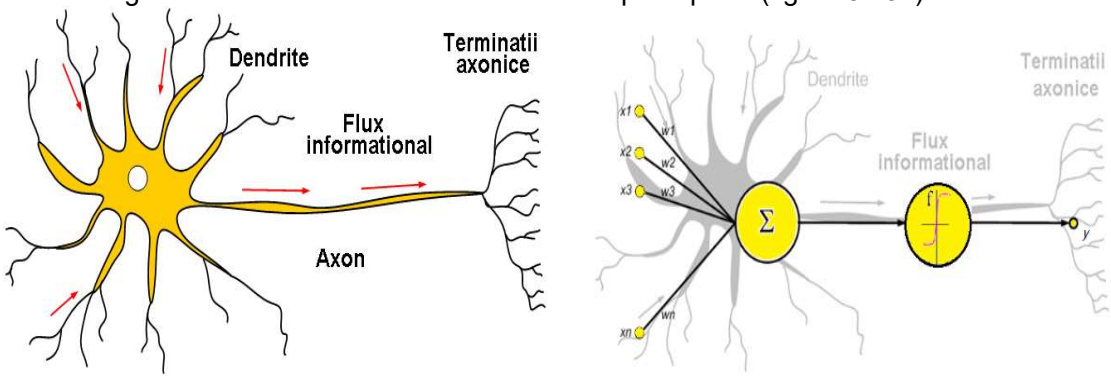

(a) (b)

Figure 5. 15. Structure of a neuron (a) biological (b) artificial

From a structural point of view, there are several types of ANNs each of them being suitable for specific purposes. One of the most used is the Feed Forward structure [133] in which neurons are organized in layers, and information flows only from input to output.

5.7.4 "FEED FORWARD" RESULTS

Given the data measured experimentally, it is obvious the opportunity to use a model based on neural networks to analyze and optimize the behavior of the human body in the driving position of a car. As input data we used:

- type of movement performed (flexion - left leg extension, flexion - right leg extension, upper limb rotation to the left, upper limb rotation to the right);
- anthropometric data (height and mass of the driver);
- stiffness of the seat.

The model based on neural networks had as output data the value of the rigidity of the muscles in the pelvic - lumbar area, (k_4) and their damping coefficient (c_4), in response to the stresses to which it is subjected. For the motion type I used the Boolean data type, and for the rest of the values, the real type. The development of the model based on the neural network was carried out in several stages:

Stage 1. Establishing the optimal structure

Taking into account the analyzed problem, a neural network with the Feed Forward structure was used. In order to establish the optimal variant, a specialized software was used to generate them based on genetic algorithms, Pythia. Figure 5.17a presents the settings for generating the structure, and figure 5.17b shows the evolution of the generation process. It is observed in figure 5.17b that the optimal structure for the neural network is composed of three layers:

- input layer - seven neurons, corresponding to the seven input data;
- a hidden layer - with five neurons;
- output layer - two neurons, corresponding to the two output data.

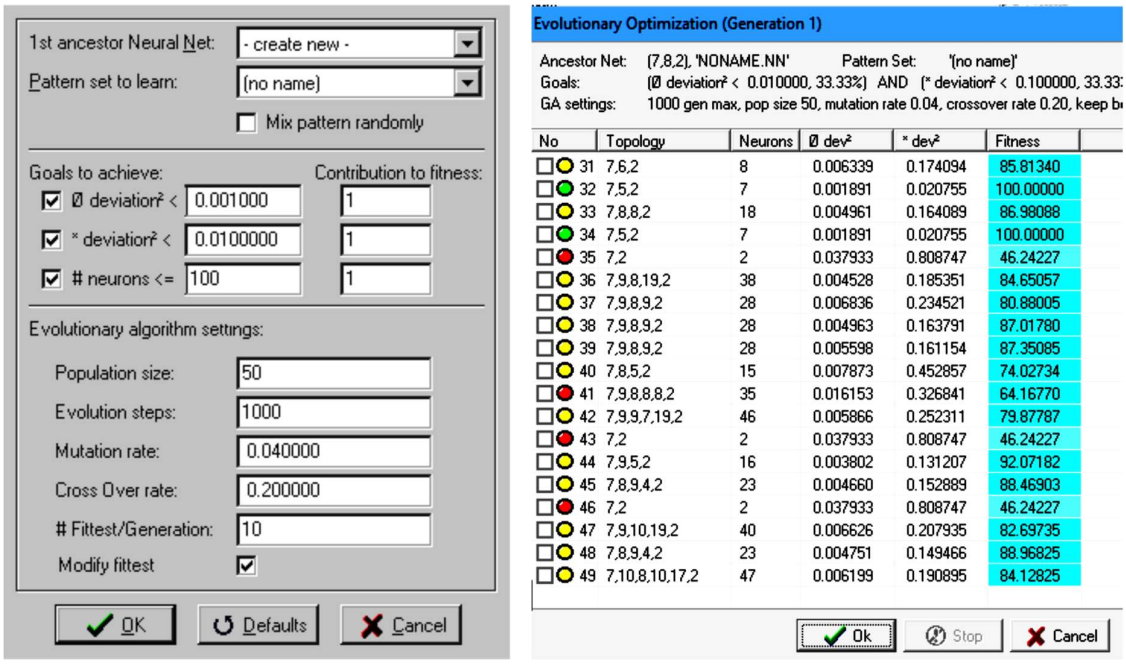

(a) (b)

Figure 5. 17. Generation of the optimal structure of the neural network
(a) settings for the genetic algorithm (b) generating the optimal structure

Stage 2. Implementation of the neural model network training and validation

The EasyNN software was used to implement the network structure and use it. This allows the organization of the input-output data sets for network training (figure 5.18a), visualizing the network and the evolution of the training error (figure 5.18b and figure 5.18c). The training rate used had a value Ra = 0.6 and a sigmoid transfer function. The value of the training error was Ea = 0.01.

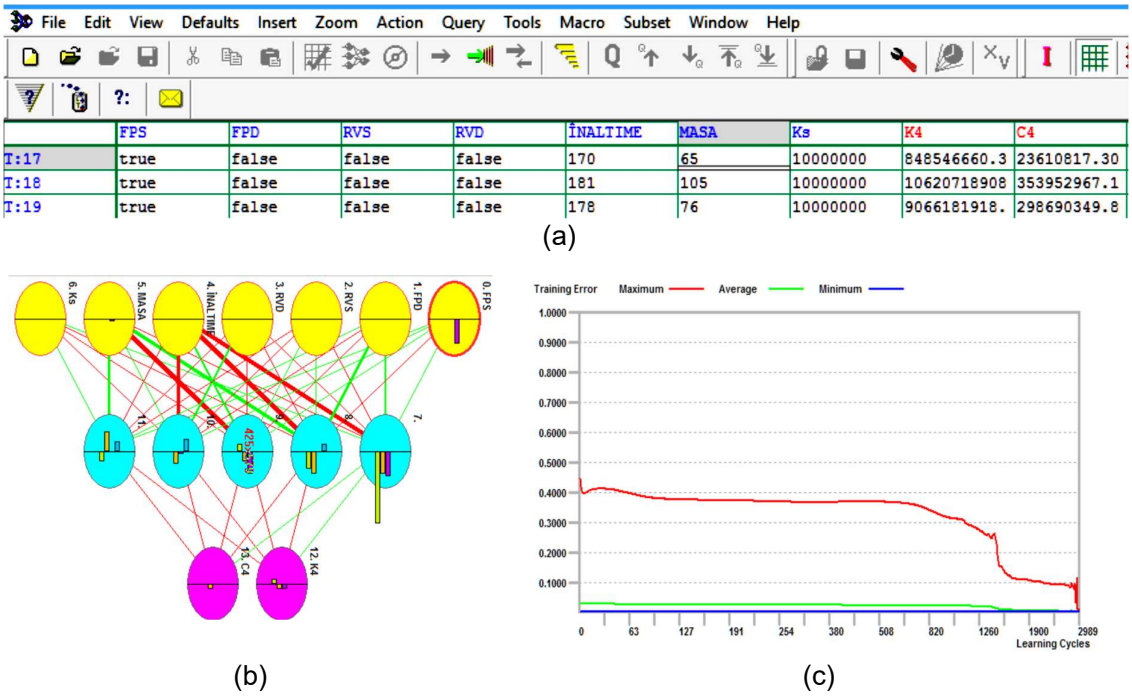

Figure 5. 18. Organization of data sets (a) for training the network (b) for viewing the network (c) evolution of the training error

Stage 3. Establishment of the most important factor of influence on k_4 and c_4 (the stiffness and damping coefficients of the muscle group in the pelvic area).

EasyNN provides information regarding the importance of graphical entries (figure 5.19).

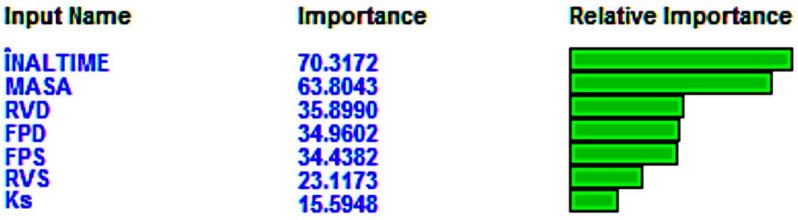

Figure 5. 19. The importance of the input data on the output data

It can be seen in figure 5.19 that the factors determined for the values k_4 and c_4 are the height and the mass of the driver respectively and that the rigidity of the seat (k_s) has a small importance in the evolution of the values k_4 and c_4.

Stage 4. Analysis of the evolution of the stiffness coefficient k_4

With the help of the proposed neural model, an analysis of the evolution of the coefficient values k_4 can be performed, in order to establish the conditions of minimum stress in the lumbar - pelvic area of the driver.

High elasticity coefficients in the lumbar area are also developed in the case of unbalanced movements (FEPS - true, RVD - true), which require the stresses of the muscle groups arranged diagonally up-down (FEPS) and left-right (RVD).

Table 5. 1. Extreme values of the stiffness coefficient k_4

k_S [N/m]	1000000		10000000	
k_4 [N/m]	min	max	min	max
	206407887,712	55042055255,024	674008,907	37744473065,758
FEPS	FALSE	TRUE	FALSE	TRUE
FEPD	FALSE	FALSE	FALSE	FALSE
RVS	FALSE	FALSE	FALSE	FALSE
RVD	FALSE	TRUE	FALSE	TRUE
HEIGHT [cm]	185	165	192	173
MASS [kg]	78	130	72	85

The built neural model allows the prediction of the k_4 values for input data different from those used to train the neural network. In this way one can appreciate the opportunity of assigning the position of driver to a certain person.

5.8 PARTIAL CONCLUSIONS

The conclusions regarding the approach of the theoretical and experimental research of the dynamics of the driver conducted in this paper, will be presented in accordance with the proposed objectives and activities.

The developed model can be used to analyze the main mechanical property of the muscular system - elasticity, during the postural behavior of the driver. The values determined for the elasticity and damping coefficients of the muscle groups have been proven to validate the area in which the active force developed at the pelvic - sacral and lumbar level has high values. This is due to the muscle groups that have their origin or insertions at the thigh, sacral and pelvic level. From a mechanical point of view, the elasticity coefficients of these muscle groups have high values justified by the ratio between the initial section of the muscle and its length.

The elaborated model can be used in the comparative analysis regarding the characteristic parameters of the driver's movements, for both professional and amateur drivers, or between different anthropometers.

Following the analysis of the second model based on the data provided by "iPi - Soft" and with the help of neural networks, we can highlight a number of conclusions:

- by using artificial neural networks models can be developed that predict the evolution of the coefficients of elasticity of the muscle groups of the drivers;
- neural modeling allows to highlight the essential elements that influence the variation of the elasticity coefficients in the overloaded areas

CHAPTER 6

GENERAL CONCLUSIONS OF BIOMECHANICAL ANALYSIS, PERSONAL CONTRIBUTIONS AND FUTURES RESEARCH DIRECTIONS

6.1 GENERAL CONCLUSIONS

Optical recording systems have an important contribution to the motion capture and analysis. The systems used require specialists for their proper functioning because they require the calibration, acquisition and interpretation of the data. For this reason, it is intended to use, in the analysis of a biomechanical system, a device with a simple interface, indicating the movements and allowing the comparison with an existing model in a data library for its correction or optimization.

Due to the reliability and the affordable price, the Kinect camera proves to be an alternative to the systems based on light markers. Using the Kinect sensor in this thesis is an accessible and efficient way to determine the kinematic and dynamic parameters of the driver. Compared to a video recording made with a normal camera, the recording made by the Kinect camera provides the values of some vectorized parameters (speed, acceleration), necessary to determine the muscular or joint stress. The Kinect sensor offers the ability to capture video data in almost any ambient light environment, based on automatic calibration with the environment.

In the chapter entitled "Structural identification of the mechanisms in the biomechanical system of the driver", the levers and joints of the human bone system in the sitting position as well as the kinetic chains that they perform are identified and analyzed from a biomechanical point of view. At the structural level, the actuation of the devices in the driving position is performed by the body based on the lever systems. The most common are those of class 2 and 3. the influence of the position of the hands on the steering wheel on the temperatures of the tegument. The positioning of the hands in the area "10 - 2" is the most unfavorable in terms of blood circulation, which is why, in all subjects, the temperature decreases, with a linear tendency, having a strong correlation with the average.

Placing the hands in the position "7 - 5" proves to be more favorable, from a thermal point of view, compared to the positioning in the area "10 - 2", the slope of the regression equations being smaller, but it represents an inconvenient position from the point of view of comfort and kinematics of the hands. The thermal analysis of the hands in the position "9 - 3" proved to be the best, the temperature variations being insignificant for 5 minutes, considering that these variations are due to the heat exchange with the outside and the thermoregulation at the finger level.

The purpose of this PhD thesis was to identify a mechanical model of the driver. For this purpose, the muscle groups were analyzed as mass - spring - damping (MSD) systems in order to establish the dynamically overloaded anatomical areas during the handling of the different devices. The way to approach the theoretical and experimental research of the

dynamics of the driver is presented in the chapter "Analysis of stresses from the biomechanical system of the driver".

The development of the recording techniques without luminous markers, of the methods of processing and filtering the images, allowed a greater accuracy of the data in the kinematic and dynamic analysis of the human movements. The use of the iPi Recorder 4.0 software offers the possibility of biomechanical analysis of the solid anatomical elements (the bone system) by identifying them at the overlap of the virtual model according to anthropometry, offering their trajectories, speeds and accelerations. The results obtained from the dynamics of the multi-body system could be used in modeling the driver's movements.

The model developed can be used to analyze the main mechanical property of the muscular system - the elasticity, during the postural behavior of the driver. The determined values of the coefficients have been proven to validate the area in which the active force developed at the pelvic - sacral - lumbar level has high values. This is due to the muscle groups that have their origin or insertions at the thigh, sacral and pelvic level. From a mechanical point of view, the elasticity coefficients of these muscle groups have high values justified by the ratio between the initial section of the muscle and its length.

The elaborated model can be used in the comparative analysis regarding the characteristic parameters of the driver's movements, for professional and amateur drivers, or between different anthropometers.

The fifth chapter addresses a method of mathematical modeling of driver dynamics. The 2 models presented in this chapter are based on the mass-spring-damping structure. Both models contain 11 kinematic elements developed (connected) based on the Voight model. The proposed models are differentiated by the connection of the muscular system in the sacrum-lumbar-pelvic area. Based on the two mathematical models, the flexion and extension movements were analyzed. The obtained results conclude that the highest values of the stiffness and damping coefficients are found in the pelvic area. These coefficients are associated with muscles with insertions on the sacral bone, iliac bone and femur. The high values recorded in this area indicate high voltages generated during the stroke. These stresses are due to the elastic forces depending on the stiffness coefficient of the muscle. In this area, the presented muscular formations have small dimensions (length and section) and generate small displacements and therefore large elastic forces.

The results obtained on the basis of the first model led to an overview of the tensions in the pelvic area. Following the results obtained from the first model, it was necessary to develop a new dynamic model MSD.

The proposed new model is also composed of 11 rigid elements, but which more accurately reproduce the system mass - spring - damping in the pelvis area. The data resulted from the second model was used as input data for a neural network of Feed Forward type. Following the training and running of the neural network, a number of conclusions can be highlighted:

- with the help of artificial neural networks, a model for k 4 and c 4 evolution can be built in the case of drivers;
- neural modeling allows to highlight the essential elements that influence the variation k_4 and c_4, namely the height and the mass of the driver;
- the neural model allows the input values to be optimized in order to obtain minimum values for k 4 and, therefore, an increased comfort at the driving position.

This paper analyzed the position of the driver from a kinematic and dynamic point of view. The experiments performed aimed to observe different problems that arise during the operation of the control devices of a vehicle. Thus, the use of some motion capture tools and motion analysis applications have proven to be efficient in the biomechanical analysis of the driver.

6.2 PERSONAL CONTRIBUTIONS

The approach of the research topic presented in the doctoral thesis was based on a series of own contributions that led to the achievement of the aimed objectives. These can be summarized as it follows:

1. Structural identification of the levers and equivalent kinematic couplings of the human body participating in the driver's position. This was realized by reducing the bone system to a system of articulated rigid bars to identify all the levers and kinematic couplings of the biomechanical system of the driver.
2. Analysis of the dependence between the kinematic parameters of the driver in the sitting position where it has been shown that increasing the absolute angle of a joint brings the body of the driver closer to the steering wheel.
3. Creating a stand that reproduces the driver's driving position in order to be able to use image recording means without being interfered with by different devices. The stand complies with the dimensions of the driving post and could be used both for the kinematic analysis of the driver and for the dynamic analysis.
4. Using the Kinovea application to observe the differences of posture in the driver's kinematics. With the help of this application we have been able to demonstrate that a high plantar pressure in the heel and metatarsal head areas can lead to a decrease in the plantar support area, which means it leads to a postural instability that causes the delay of operating the vehicle’s pedals.
5. Use of the Pearson statistical correlation method to establish a correlation between the angles of the joints of the lower limb in both "no heel" and "with heel" cases. For both cases, this correlation method has shown that the flexions and extensions of the driver's knee are in close connection.
6. Use of the Kinect sensor to capture the driver's movement. I made captures with the help of 2 Kinect sensors without any delays between the frames of the two recordings, which were able to provide more precise data on the driver's movement than when using a single Kinect sensor.
7. ANOVA statistical analysis of the temperature of the tegument of the driver's hands for positioning in various areas of the steering wheel. This was done with the help of a thermovision camera on a sample of 10 subjects and pointed out that by placing the hands on the steering wheel in the zone "9 - 3" of the hourly dial the temperature of the hands does not decrease significantly and there is no possibility of blood vasoconstriction.
8. Use of an application used in video animation to collect driver movement data. In this regard, the iPi - Soft application has proven to be very efficient without using luminous markers to identify anatomical elements or joints.
9. Determination of the trajectories, speeds, accelerations and forces developed at the level of the anatomical elements of the driver during the flexion - extension movements of the lower limbs and adduction - abduction at the level of the upper limbs.
10. Using the Pearson statistical method to observe the correlation between the forces developed in the lumbar area of the driver and the rest of the forces developed at the level of the anatomical elements. It was found that there is a very good correlation between the muscular forces in the lumbar area and the muscular forces developed at the thigh and hip level when the driver operates the pedal. There was also a moderate correlation between the muscular forces in the lumbar area and the muscular forces in the scapular area and the arm area when turning the steering wheel by 90 °.
11. Develop a script that solves systems of 22 equations with 22 unknowns using the Matlab application in order to determine the stiffness and damping coefficients of the muscle groups.
12. Development of dynamic models of mass-spring-damping type of the driver that lead to the determination of the coefficients of stiffness and damping of the human muscles.

Following these models, it was found that the highest values of the stiffness and damping coefficients are specific to the lumbar - pelvic area, regardless of the seat's stiffness.

13. Use of neural networks to predict the stiffness coefficients of human muscles in order to assess the attribution of the position of driver to a certain anthropometry.

6.3 FUTURE RESEARCH DIRECTIONS

This doctoral thesis opens a series of future research directions for the biomechanical analysis of the driver. In this regard, I propose:

1. Developing a more complex kinematic analysis system in order to determine the active space of the driver.
2. Developing new dynamic models of mass-spring-damping type for both sitting and orthostatic position in order to eliminate the positions that have pathological implications.
3. Simulation of models using the ADAMS application.
4. Use of neural networks to determine optimal positions of different anthropometers for certain human positions of work.
5. Developing a model of car seat that will provide increased comfort to the driver in the optimal position.
6. Connecting more than 2 Kinect sensors on the same interface for collecting the most accurate data for biomechanical analysis.

SCIENTIFIC RESULTS

Books published

1. Daniel Ganea, Elena Mereuță, **Valentin Amorțilă**, INTRODUCERE ÎN BIOMECANICA CORPULUI UMAN, Editura University Press, Galați, 2019, ISBN 978-606-696-175-2

Publications in WoS indexed journals

1. Daniel Ganea, **Valentin Amorțilă**, Elena Mereuță, Eugen Rusu, A JOINT EVALUATION OF THE WIND AND WAVE ENERGY RESOURCES CLOSE TO THE GREEK ISLANDS Sustainability 9 (6), 1025 https://doi.org/10.3390/su9061025, Factor de impact: 1,789
2. Costel Humelnicu, Sorin Ciortan, **Valentin Amorțilă**, ARTIFICIAL NEURAL NETWORK-BASED ANALYSIS OF THE TRIBOLOGICAL BEHAVIOR OF VEGETABLE OIL–DIESEL FUEL MIXTURES, Lubricants 7 (4), 32, https://doi.org/10.3390/lubricants7040032

Publications in SCOPUS indexed journals

1. **Valentin Amorțilă**, Elena Mereuță, Daniel Ganea, Costel Humelnicu, Sorin Ciortan, AUTO TRANSPORTATION-AN IMPORTANT FACTOR IN POLLUATION GROWTH AND IN ATMOSPHERIC CHANGES, DOI: 10.5593/sgem2018/4.2/S19.046, International Multidisciplinary Scientific GeoConference Surveying Geology and Mining Ecology Management, SGEM18(4.2), pp. 349-356, DOI: 10.5593/sgem2018/4.2/S19.046

2. **Valentin Amorțilă**, Elena Mereuță, Silvia Vereșiu, Mădălina Rus, Costel Humelnicu, POSITIONING STUDY OF DRIVER'S HANDS IN CERTAIN AREAS OF THE STEERING WHEEL, MATEC Web of Conferences 178, 06014

3. **Valentin Amorțilă**, Elena Mereuță, Costel Humelnicu, Mihai Gingărașu, DRIVER'S BIOMECHANICS INFLUENCE ON AIR POLLUTION, International Multidisciplinary Scientific GeoConference Surveying Geology and Mining Ecology Management, SGEM18(4.3), pp. 251-258;

4. **Valentin Amorțilă**, Elena Mereuță, Daniel Ganea, Mădălina Rus, Silvia Vereșiu, EXPERIMENTAL TEST FOR EXHAUST GASES RECIRCULATION SYSTEM DIAGNOSTIC BASED ON GAS INDEX COEFFICIENT, International Multidisciplinary Scientific GeoConference Surveying Geology and Mining Ecology Management, SGEM17(41), pp. 433-440

5. **Valentin Amorțilă**, Elena Mereuță, Costel Humelnicu, Mihai Gingărașu, THE VIBRATION AND NOISE POLLUTION'S IMPACT ON THE DRIVER, International Multidisciplinary Scientific GeoConference Surveying Geology and Mining Ecology, SGEM19(4.1), pp. 1143-1150; ISBN 978-619-7408-83-6

6. Silvia Vereșiu, Elena Mereuță, Mădălina Rus, Daniel Ganea, **Valentin Amorțilă**, FORECAST OF A QUALITY INDICATOR IN ACADEMIC ACTIVITY USING STATISTICAL METHODS, MATEC Web of Conferences 112, 08008

7. Costel Humelnicu, **Valentin Amorțilă**, Mihai Gingărașu, Elena Mereuță, DAMAGING BY TRIBO-FATIGUE AND TEST RIG DESIGN, International Multidisciplinary Scientific GeoConference Surveying Geology and Mining Ecology Management, SGEM18(4.3), pp. 235-242

8. Costel Humelnicu, **Valentin Amorțilă**, Elena Mereuță, NEURAL NETWORKS AS OPTIMIZATION TOOLS FOR FUEL CONSUMPTION, International Multidisciplinary Scientific GeoConference Surveying Geology and Mining Ecology Management, SGEM18(4.2), pp. 531-537

9. Daniel Ganea, Elena Mereuță, Silvia Vereșiu, Mădălina Rus, **Valentin Amorțilă**, EXPERIMENTAL TESTS FOR FOOT PRESSURE ANALYSIS DURING ORTHOSTATIC POSITION AND GAIT, MATEC Web of Conferences 112, 08009

10 Daniel Ganea, Elena Mereuță, Silvia Vereșiu, Mădălina Rus, **Valentin Amorțilă**, ANALYSIS OF REACTION FORCES IN HUMAN ANKLE JOINT DURING GAIT, MATEC Web of Conferences 112, 07019

11. Mihai Gingărașu, Elena Mereuță, **Valentin Amorțilă**, Costel Humelnicu, THE INFLUENCE OF VEHICLE DIAGNOSIS ON REDUCING GAS EMISSIONS THAT AFFECTS THE EARTH'S CLIMATE SYSTEM, International Multidisciplinary Scientific GeoConference Surveying Geology and Mining Ecology Management, SGEM19(4.1), pp. 1109-1115; ISBN 978-619-7408-83-6

12 Costel Humelnicu, Elena Mereuță, **Valentin Amorțilă**, Mihai Gingărașu, REDUCING THE AIR POLLUTION IMPACT OF THE RECYCLED AUTO VEHICLES, International Multidisciplinary Scientific GeoConference Surveying Geology and Mining Ecology Management, SGEM19(4.1), pp. 1053-1060; ISBN 978-619-7408-83-6

13. Costel Humelnicu, **Valentin Amorțilă**, Elena Mereuță, FATIGUE LIFE INVESTIGATION ON A MAC ENGINE PISTON, MATEC Web of Conferences 178, 06013

Publications under indexing SCOPUS

14. **Valentin Amorțilă**, Elena Mereuță,, Costel Humelnicu, Mihai Gingărașu, Monica Novetschi, CONTROVERSY ABOUT CAR POLLUTION: THE ELECTRIC VEHICLE OR THE CLASSIC VEHICLE?, International Multidisciplinary Scientific GeoConference: SGEM 19 (4.2) pp. 193-200; ISBN 978-619-7408-98-0

15. Costel Humelnicu, Elena Mereuță, **Valentin Amorțilă**, Mihai Gingărașu, FATIGUE POLYMERIC MATERIALS – AIR POLLUTION FACTOR, International Multidisciplinary Scientific GeoConference: SGEM 19 (4.2) pp. 221-228; ISBN 978-619-7408-98-0

16. Mihai Gingărașu, Elena Mereuță, Valentin Amorțilă, Costel Humelnicu, THE INFLUENCE OF VEHICLE STEERING SYSTEM MISSALIGNMENT ON THE ENVIRONMENT, International Multidisciplinary Scientific GeoConference: SGEM 19 (4.2) pp. 295-302; ISBN 978-619-7408-98-0

REFERENCES

[26] S. Schmidt, M. Amereller, M. Franz, R. Kaiser, and A. Schwirtz, “A literature review on optimum and preferred joint angles inautomotive sitting posture,” *Appl. Ergon.*, vol. 45, no. 2 PB, pp. 247–260, 2014.

[66] H. Loeb *et al.*, “Automated recognition of rear seat occupants’ head position using Kinect™ 3D point cloud.,” *J. Safety Res.*, vol. 63, pp. 135–143, 2017.

[67] K. M. Lion, K. H. Kwong, and W. K. Lai, “Smart speed bump detection and estimation with kinect,” in *Proceedings - 2018 4th International Conference on Control, Automation and Robotics, ICCAR 2018*, 2018, pp. 465–469.

[68] E. Frigieri, G. Borghi, R. Vezzani, and R. Cucchiara, “Fast and accurate facial landmark localization in depth images for in-car applications,” in *Lecture Notes in Computer Science (including subseries Lecture Notes in Artificial Intelligence and Lecture Notes in Bioinformatics)*, 2017, vol. 10484 LNCS, pp. 539–549.

[69] A. Turpen, “Toyota using DARV with Microsoft Kinect to combat distracted driving,” 2013. [Online]. Available: http://www.carnewscafe.com/2013/11/toyota_darv_microsoft_kinect/. [Accessed: 26-Dec-2019].

[70] R. D. Armin Ambuhl, Sergei Lupashin, “Interaction with a Quadrotor via the Kinect, ETH Zurich - YouTube,” 2011. [Online]. Available: https://www.youtube.com/watch?v=A52FqfOi0Ek. [Accessed: 26-Dec-2019].

[73] N. Eric and J. W. Jang, “Kinect depth sensor for computer vision applications in autonomous vehicles,” in *International Conference on Ubiquitous and Future Networks, ICUFN*, 2017, pp. 531–535.

[74] G. Borghi, R. Gasparini, R. Vezzani, and R. Cucchiara, “Embedded recurrent network for head pose estimation in car,” in *IEEE Intelligent Vehicles Symposium, Proceedings*, 2017, pp. 1503–1508.

[75] F. Schlagenhauf, P. P. Sahoo, and W. Singhose, “Comparison of single-kinect and dual-kinect motion capture of upper-body joint tracking,” in *2017 Asian Control Conference, ASCC 2017*, 2018, vol. 2018-January, pp. 256–261.

[76] P. Chiariotti, G. Battista, M. Ettorre, and P. Castellini, “Average acoustic beamforming in car cabins: An automatic system for acoustic mapping over 3D surfaces,” *Appl. Acoust.*, vol. 129, pp. 47–63, Jan. 2018.

[77] O. Ciobanu and G. Ciobanu, “An application of kinect-based 3D scanning in biomedical engineering,” in *RAD Conference Proceedings*, 2016, vol. 1, pp. 183–186.

[80] D. Ganea, “Studiul dinamicii lanţului cinematic al membrului inferior uman cu sistem de camere kinect,” *Teza Dr.*, vol. Teză de do, 2013.

[81] Z. Gao, Y. Yu, Y. Zhou, and S. Du, “Leveraging Two Kinect Sensors for Accurate Full-Body Motion Capture,” *Sensors*, vol. 15, no. 9, pp. 24297–24317, Sep. 2015.

[82] T. B. Moeslund, A. Hilton, and V. Krüger, “A survey of advances in vision-based human motion capture and analysis,” *Comput. Vis. Image Underst.*, vol. 104, no. 2–3, pp. 90–126, Nov. 2006.

[83] “Motion Capture Cameras | The Full Range from Vicon.” [Online]. Available: https://www.vicon.com/hardware/cameras/. [Accessed: 28-Dec-2019].

[84] “Xsens MTi 100-series | Geo-matching.com.” [Online]. Available: https://geo-matching.com/inertial-measurement-units-imus/mti-100-series. [Accessed: 28-Dec-2019].

[85] H. Zhang, “Using Microsoft Kinect Sensor in Our Research - PDF Free Download,” 2011. [Online]. Available: http://docplayer.net/30257750-Using-microsoft-kinect-sensor-in-our-research.html. [Accessed: 09-Dec-2019].

[86] “Microsoft confirme l’arrêt de Kinect.” [Online]. Available: https://fr.ign.com/xbox-

one/30701/news/microsoft-confirme-larret-de-kinect. [Accessed: 28-Dec-2019].
[87] A. Jana, “Kinect for Windows SDK Programming Guide Chapter No. 1 ‘Understanding the Kinect Device,’” 2012.
[88] K. Khoshelham and S. O. Elberink, “Accuracy and resolution of kinect depth data for indoor mapping applications,” *Sensors*, vol. 12, no. 2, pp. 1437–1454, Feb. 2012.
[89] “Fitnect - Interactive Virtual Fitting / Dressing Room application - YouTube,” 2011. [Online]. Available: https://www.youtube.com/watch?v=1jbvnk1T4vQ. [Accessed: 28-Dec-2019].
[90] F. T. Cerezo, “3D Hand and Finger Recognition using Kinect,” *unpublished*, 2011.
[91] I. Oikonomidis, N. Kyriazis, and A. A. Argyros, “Efficient model-based 3D tracking of hand articulations using kinect,” in *BMVC 2011 - Proceedings of the British Machine Vision Conference 2011*, 2011.
[92] “E3 2011: Kinect Fun Labs Election: Keyboard Anywhere - YouTube.” [Online]. Available: https://www.youtube.com/watch?v=4STUGl-YHDc. [Accessed: 09-Dec-2019].
[93] “Kinect Fun Labs Election: Keyboard Anywhere - YouTube,” 2010. [Online]. Available: https://www.youtube.com/watch?v=4STUGl-YHDc. [Accessed: 28-Dec-2019].
[94] J. L. C.-E. C. H. Guzmán-Valdivia, A. Blanco-Ortega, M.A. Oliver-Salazar, “Therapeutic Motion Analysis of Lower Limbs Using Kinovea,” *Int. J. Soft Comput. Eng.*, vol. Volume-3, no. Issue-2, 2013.
[95] S. H. Elwardany, W. H. El-Sayed, and M. F. Ali, “Validity of Kinovea Computer Program in Measuring Cervical Range of Motion in Frontal Plane,” 2016.
[96] “Kinovea Basic tools Part 1.” [Online]. Available: https://www.youtube.com/watch?v=20wOlps_Nj0. [Accessed: 28-Dec-2019].
[97] “iPi Motion Capture Version 4.” [Online]. Available: http://ipisoft.com/store/version-4-0/. [Accessed: 09-Dec-2019].
[98] E. Mereuta, “Mecanisme,” *Ed. Evrika*, pp. 1–229, 2001.
[99] J. L. C.-E. C. H. Guzmán-Valdivia, A. Blanco-Ortega, M.A. Oliver-Salazar, “Therapeutic Motion Analysis of Lower Limbs Using Kinovea,” *Int. J. Soft Comput. Eng.*, vol. 3, no. 2, 2013.
[100] V. Amortila, E. Mereuta, C. Humelnicu, and M. Gingarasu, “Driver’s biomechanics influence on air pollution,” in *International Multidisciplinary Scientific GeoConference Surveying Geology and Mining Ecology Management, SGEM*, 2018, vol. 18, no. 4.3, pp. 251–258.
[101] D. Ganea, E. Mereuta, S. Veresiu, M. Rus, and V. Amortila, “Experimental tests for foot pressure analysis during orthostatic position and gait,” in *MATEC Web of Conferences*, 2017, vol. 112.
[102] D. Walton and J. A. Thomas, “Naturalistic observations of driver hand positions,” *Transp. Res. Part F Traffic Psychol. Behav.*, vol. 8, no. 3, pp. 229–238, 2005.
prediction in locomotion.,” *J. Biomech.*, vol. 14, no. 11, pp. 793–801, 1981.
[121] T. W. Lu, J. J. O’Connor, S. J. G. Taylor, and P. S. Walker, “Validation of a lower limb model with in vivo femoral forces telemetered from two subjects,” *J. Biomech.*, vol. 31, no. 1, pp. 63–69, Nov. 1997.
[122] A. M. Kese, *Biomecanica aparatului locomotor*. Craiova: Editura Universitaria, 2012.
[123] A. Gagea, *BIOMECANICĂ ANALITICĂ*. București, 2006.
[124] M.R. Pierrynowski, “Analytic Representation of Muscle Line of Action and Geometry - Technische Informationsbibliothek (TIB),” 1995. [Online]. Available: https://www.tib.eu/en/search/id/BLCP%3ACN005849433/Analytic-Representation-of-Muscle-Line-of-Action/. [Accessed: 15-Jan-2020].
[125] M. D. Klein Horsman, H. F. J. M. Koopman, F. C. T. van der Helm, L. P. Prosé, and H. E. J. Veeger, “Morphological muscle and joint parameters for musculoskeletal modelling of the lower extremity,” *Clin. Biomech.*, vol. 22, no. 2, pp. 239–247, 2007.
[126] A.A. Picu, “Modelarea biomecanică neliniară a dinamicii corpului uman sub acţiunea vibraţiilor transmise,” Universitatea „Dunărea de Jos” Galaţi, 2010.

[127] J. Babic and J. Lenarcic, “In vivo determination of triceps surae muscle-tendon complex viscoelastic properties,” *Eur. J. Appl. Physiol.*, vol. 92, no. 4–5, pp. 477–484, Aug. 2004.
[128] B. Daniela Mariana, “TEZĂ DE ABILITARE Cercetări aplicative în analiza și modelarea biosistemelor umane cu scopul creșterii calității vieții Domeniul: Inginerie mecanică Autor: Conf. dr. ing.”
[129] A. A. Nikooyan and A. A. Zadpoor, “Mass-spring-damper modelling of the human body to study running and hopping-an overview,” *Proceedings of the Institution of Mechanical Engineers, Part H: Journal of Engineering in Medicine*, vol. 225, no. 12. pp. 1121–1135, Dec-2011.
[130] A. A. Biewener, “Locomotion as an emergent property of muscle contractile dynamics,” *Journal of Experimental Biology*, vol. 219, no. 2. Company of Biologists Ltd, pp. 285–294, 01-Jan-2016.
[131] F. Bausic, “CONSIDERAȚII ASUPRA UNUI MODEL DINAMIC CU 15 GRADE DE LIBERTATE AL MÂINII UMANE.”
[132] A. Afkar, I. Javanshir, M. T. Ahmadian, and H. Ahmadi, “Optimization of a passenger occupied seat with suspension system exposed to vertical vibrations using genetic algorithms,” • *J. Vibroengineering 15(2)979-991*, 2013.
[133] C. Humelnicu, S. Ciortan, and V. Amortila, “Artificial neural network-based analysis of the tribological behavior of vegetable oil-diesel fuel mixtures,” *Lubricants*, vol. 7, no. 4, Apr. 2019.